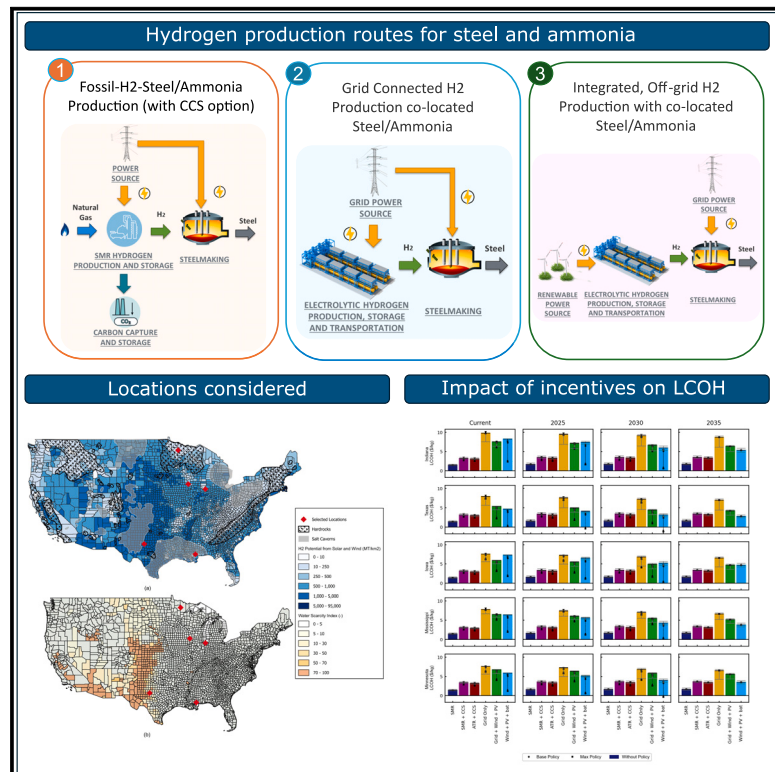


Techno-economic analysis of low-carbon hydrogen production pathways for decarbonizing steel and ammonia production

Graphical abstract



Highlights

- This study analyzes the economics of low-carbon hydrogen production for steel and ammonia
- IRA incentives make off-grid electrolysis competitive with SMR/ATR+CCS with current costs
- Future cost reductions might allow electrolysis to be competitive without incentives
- Strong renewable resources, low-cost hydrogen storage, and proximity to feedstocks are key

Authors

Evan P. Reznicek, Mariya N. Koleva, Jennifer King, ..., Hanna Breunig, Fabian Rosner, João Onofre Pereira Pinto

Correspondence

evan.reznicek@nrel.gov (E.P.R.), mariya.koleva@nrel.gov (M.N.K.), jennifer.king@nrel.gov (J.K.)

In brief

Reznicek et al. analyze the economics of multiple routes of hydrogen production for steel and ammonia production within the US in the context of IRA incentives. They find that these incentives could make renewable-powered, behind-the-meter electrolytic hydrogen production economically competitive with fossil fuel-based hydrogen production with current technology performance and costs in multiple US locations and that renewable-powered, behind-the-meter electrolytic hydrogen production might be cost competitive with fossil-based routes in some locations by 2035 even without incentives.



Article

Techno-economic analysis of low-carbon hydrogen production pathways for decarbonizing steel and ammonia production

Evan P. Reznicek,^{1,*} Mariya N. Koleva,^{1,*} Jennifer King,^{1,6,*} Matthew Kotarbinski,¹ Elenya Grant,¹ Sanjana Vijayshankar,¹ Kaitlin Brunik,¹ Jared Thomas,¹ Abhineet Gupta,¹ Steven Hammond,¹ Vivek Singh,¹ Richard Tusing,¹ Pingping Sun,² Kyuha Lee,² Amgad Elgowainy,² Hanna Breunig,³ Fabian Rosner,^{3,5} and João Onofre Pereira Pinto⁴

¹National Renewable Energy Laboratory, Golden, CO 80401, USA

²Argonne National Laboratory, Lemont, IL 60439, USA

³Lawrence Berkeley National Laboratory, Berkeley, CA 94720, USA

⁴Oak Ridge National Laboratory, Oak Ridge, TN 37830, USA

⁵Renewable Energy and Chemical Technologies (REACT) Lab, Department of Civil and Environmental Engineering, University of California, Los Angeles, Los Angeles, CA 90095, USA

⁶Lead contact

*Correspondence: evan.reznicek@nrel.gov (E.P.R.), mariya.koleva@nrel.gov (M.N.K.), jennifer.king@nrel.gov (J.K.)

<https://doi.org/10.1016/j.crsus.2025.100338>

SCIENCE FOR SOCIETY The last several years have seen tremendous growth in the interest in hydrogen as a means for reducing emissions in hard-to-decarbonize industrial sectors. Legislation like the Bipartisan Infrastructure Law of 2021 and the enactment of incentives for clean hydrogen production in the Inflation Reduction Act (IRA) of 2022 have only accelerated this increased interest. When, where, and how clean hydrogen production will provide economically attractive opportunities for industrial decarbonization remains unclear in part due to uncertainty in parameters such as future electrolyzer capital costs, electricity prices, natural gas prices, electrolyzer durability and flexibility, the cost and time frame for establishing large-scale grid interconnections for electrolysis, and the availability and cost of hydrogen storage. This study provides an extensive analysis of the economics of clean hydrogen production for decarbonizing steelmaking and ammonia synthesis via three key production routes: (1) fossil-based routes including steam methane reforming (SMR) with and without carbon capture and sequestration (CCS) and autothermal reforming (ATR) with CCS, (2) grid-powered electrolysis (with and without on-site renewables), and (3) off-grid renewable-driven electrolysis. We perform sensitivity and scenario analysis on parameters such as electrolyzer costs, natural gas costs, and location, and we use state-of-the-art projections for future technology costs vetted by experts within the US Department of Energy (DOE) and across US national laboratories. This work does not reflect policy or provide policy guidance but makes preliminary assumptions that we believe are consistent with the final regulations relating to the credit for the production of clean hydrogen (45V, clean hydrogen production credit) and the energy credit, as established and amended by the IRA of 2022, respectively. The results of this study can inform government, industry, and the public about when, where, and how low-carbon hydrogen production can potentially reduce emissions of steelmaking and ammonia synthesis.

SUMMARY

Low-carbon hydrogen can play a key role in decarbonizing steel and ammonia production. Here, we report a techno-economic and life-cycle emissions analysis of different hydrogen production routes for steelmaking via direct reduced iron-electric arc furnace and ammonia synthesis for five locations with estimated technological progress through 2035 and considering a range of Inflation Reduction Act (IRA) tax credits. Our results show that these credits can make off-grid renewable-driven electrolytic hydrogen production competitive with fossil-based routes for decarbonizing steel and ammonia in several locations within the current decade and that off-grid electrolytic hydrogen production could potentially be cost competitive with fossil-based routes in Texas and Minnesota by 2035 even without incentives. Furthermore, with maximum IRA tax incentives, off-grid electrolytic hydrogen production is competitive with fossil-based hydrogen production routes



with current technology costs. Strong renewable energy resources, access to low-cost hydrogen storage, and proximity of process feedstocks are all critical for enabling these decarbonization opportunities.

INTRODUCTION

Reducing industrial emissions is critical for achieving a net-zero economy. Industry is currently responsible for approximately 30% of greenhouse gas (GHG) emissions in the US. In 2021, cement, iron and steel, petrochemicals, and ammonia production were responsible for 11%, 10%, 9%, and 3%, respectively, representing significant contributions to climate change.¹ Industry accounts for a substantial amount of global emissions as well, with steel production responsible for approximately 7%–9% of global GHG emissions in 2020.^{2,3} Today, 70% of the global crude steel production is based on blast furnace-basic oxygen furnace (BF-BOP), 22% is produced via scrap-based electric furnace,³ 7% is produced with direct reduced iron-electric arc furnace (DRI-EAF) using natural gas, and the remaining is based on other technologies.⁴ In 2022, the US produced 94.7 million net tons of raw steel.⁵ Approximately 70% of US steel production is made through the EAF route. 90% of EAF steel in the US uses scrap steel as a feedstock, and 10% uses DRI as a feedstock.⁶ As a result, DRI-EAF currently accounts for only 7% of US steel-making. Iron ore-based steelmaking processes comprise the other 30% of US steel production, however, and these processes still heavily rely on emissions-intensive fossil fuels.⁶ The International Energy Agency (IEA) recently identified renewable electricity, hydrogen, and carbon capture and sequestration (CCS) as primary focus areas for decreasing emissions associated with steelmaking.⁷ Constructing new BFs with CCS has seen limited success in practice, and retrofitting old BFs with CCS faces practical challenges due to the many and variable CO₂ emission points.³ Electrowinning, on the other hand, is a novel, lower technology readiness level (TRL) technology that is expected to reach commercial readiness in the long term³ and is thus unlikely to contribute to steel decarbonization within the next decade. DRI-EAF with hydrogen represents a lower-risk alternative because it is already performed so widely with natural gas. Switching steel production entirely to a DRI-EAF process using low-carbon hydrogen and electricity could reduce more than 80% of the US average GHG emissions in the steel industry.⁸

These same hybrid renewable-hydrogen plants can also serve as the foundation to decarbonize ammonia production. Despite its lower contribution to global GHG emissions (approximately 2%⁹), ammonia production is considered a readily achievable target because the Haber-Bosch process already uses hydrogen derived from steam methane reforming (SMR) as a feedstock. The main applications for ammonia include fertilizer production and as a feedstock in the chemicals industry. In 2022, the ammonia production in the US was estimated at roughly 13 million metric tons (MMTs).¹⁰ Most of this production—approximately 31%, or roughly 4 MMTs—was for urea, a nitrogen-based fertilizer.¹¹ Ammonia could also be valuable as a hydrogen or energy carrier due to its physical properties and the existing expertise in handling, storing, and transporting ammonia.^{12,13} It could therefore help drive the decarbonization of both industrial and

energy sectors simultaneously. Ammonia is primarily produced via the Haber-Bosch process, where nitrogen reacts with hydrogen at high temperatures and pressures with the aid of a metal catalyst. Because the hydrogen for ammonia production is currently generated from SMR, which is an emissions-intensive process (approximately ~8–11 kg CO₂e per kg H₂¹⁴), it carries a substantial emissions footprint into the ammonia process. Consequently, employing clean hydrogen could dramatically reduce ammonia's emissions, which can approach near zero if the energy used for the hydrogen production is renewable.

Decarbonizing steel and ammonia production using hydrogen from renewably powered electrolysis is an attractive prospect for several reasons. The rapid cost reductions renewable technologies have experienced during the last two decades have enabled their accelerated deployment worldwide,¹⁵ and the anticipation that these cost reductions will continue in the future is driving a global effort to deploy renewable electricity to decarbonize sectors including transportation, industry, buildings, and agriculture.¹⁶ The global weighted average total installed costs for utility-scale solar photovoltaic (PV) and land-based wind projects have decreased by 82% and 35%, respectively, between 2010 and 2021.¹⁵ Analyses have projected substantial cost reduction potential for water electrolyzers,^{17–21} and DOE is targeting uninstalled proton exchange membrane (PEM) and alkaline electrolyzer (AEL) costs of \$150/kW within a decade,^{22,23} resulting in a 10-fold cost reduction. Similarly, the Danish Energy Agency estimates that PEM electrolyzers will reduce from 1,200 euro/kW in 2020 to 300 euro/kW in 2050 at a scale of 1 GW.²⁴ Further, the recently enacted IRA offers significant tax credits for renewable, clean hydrogen production and CCS projects.²⁵ Hydrogen production via renewable-driven electrolysis is modular, replicable, and scalable and can provide nearly carbon-free electricity and hydrogen feedstock to industries. Minimizing or eliminating grid emissions could enable low-carbon hydrogen production derived from grid-powered electrolysis. This low-carbon hydrogen production could contribute to economy-wide decarbonization because hydrogen can serve a diverse range of applications beyond steel and ammonia, such as long-distance and heavy-duty transportation and seasonal grid energy storage.²⁶

A number of recent publications have focused on assessing the techno-economic viability of green steel and ammonia using clean hydrogen. Efforts have applied analytical,^{27,28} modeling,^{29–32} simulation,^{8,33–35} optimization, and machine learning³ approaches for conducting techno-economic analyses (TEA). Numerous works have focused on the life-cycle assessment (LCA) of different pathways to achieve decarbonization in ammonia^{8,36,37} or steelmaking^{28,38} industries; however, to the best of our knowledge, the work presented here is the first to provide a holistic TEA of purpose-built, tightly coupled renewable-hydrogen-industrial systems that considers incentives, regional material and energy resource availability, and GHG emissions for different grid and system configurations in the US.

This study presents the modeling methodology and TEA of hybrid renewable and hydrogen production plants for industrial

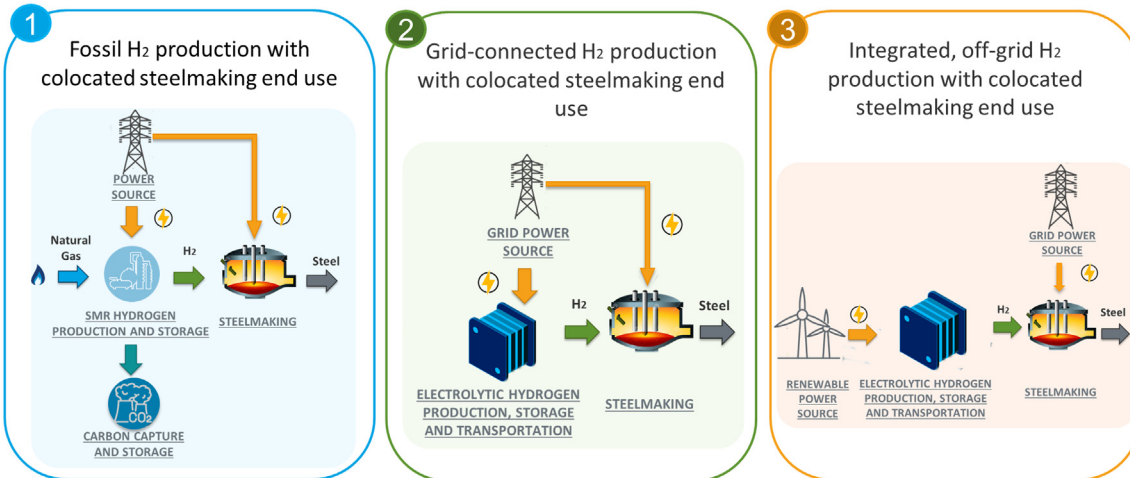


Figure 1. Hydrogen production routes considered in this analysis

Left to right: SMR with and without CCS, grid-connected electrolysis cases (some of which include on-site wind and optional solar PV), and off-grid electrolysis cases. Transportation of hydrogen to geologic storage, where available, and CO₂ transportation for sequestration are considered. This example is illustrated for steelmaking end use, but the same configurations apply for ammonia applications. Image credits: Getty Images 1303567210,⁴⁴ Getty Images 1337649626,⁴⁵ Getty Images 1555533327,⁴⁶ Phoenix Equipment Corporation,⁴⁷ and DreamsTime.⁴⁸

processes, including steel production at 1 MMTs per year and ammonia production at 0.3 MMTs per year, which are approximate average commercial plant sizes in the US.^{39–41} We consider multiple renewable and grid-connectivity configurations for electrolytic hydrogen production and compare these to fossil fuel-based hydrogen production pathways, including SMR with and without CCS and autothermal reforming (ATR) with CCS. The study considers five diverse locations in the US with unique renewable and hydrogen storage resources. It estimates cost and emissions over time, considering projections of how renewable and hydrogen production technology performance and cost might change in the coming years. We perform sensitivity and scenario analysis to quantify the potential impacts of considerations such as policy and incentives, technology cost, storage requirements, electrolyzer degradation, grid energy prices, and natural gas prices. The detailed results provide insight into the potential trajectories of different hydrogen production routes for low-carbon steel and ammonia production accounting for the impacts of policies and incentives, future costs, and location-specific design considerations. Additionally, the modeling framework used in this study has been published as an open-source tool for public and private stakeholders to use in assessing the economics of hybrid renewable-hydrogen plants for electricity production, green hydrogen production, and industrial end-use applications.

RESULTS

This study analyzes the economics of hydrogen-fueled steel and ammonia production via three hydrogen production routes. Figure 1 depicts a simplified diagram of these major scenarios. All production routes employ hydrogen within the shaft furnace for steel production, as depicted in Figure S1.³⁵ For each production route, the system boundary encompasses the hydrogen produc-

tion technology (SMR, ATR, or electrolysis), any CCS required, hydrogen storage (compressed overground, salt caverns, or lined rock caverns) and transport, and the steel or ammonia production facility. For production route one, we consider three fossil-fueled routes: SMR, SMR with CCS, and ATR with CCS, and the latter two include region-specific carbon transportation and injection costs. Production route two consists of two grid-driven electrolysis routes: grid only and grid connected with on-site wind and solar PV, the capacities of which are parametrically optimized relative to the electrolyzer capacity. The benefits of adding on-site renewables include potential cost reductions relative to grid electricity and easy opportunities to take advantage of renewable production and investment tax credits (ITCs). Supplementing renewables with power from the grid enables higher annual electrolyzer utilization (capacity factor) and facilitates steady-state hydrogen delivery without the need for seasonal hydrogen storage. This contrasts with off-grid (sometimes referred to as “behind-the-meter”) configurations where electrolyzers generally follow the highly variable signal of the renewable source and require seasonal storage to achieve steady-state delivery year-round. None of the grid-connected cases in this study consider the impacts of power purchase agreements or energy attribute certificates, which might be required by the US Department of the Treasury for hydrogen producers to qualify for incentives such as IRA hydrogen production tax credits (PTCs) based on recently proposed regulations⁴²; instead, we estimate future grid industrial retail electricity prices for a future grid scenario consistent with achieving a decarbonized US grid by 2035.⁴³ Note S3 provides more details on this study’s assumptions regarding tax incentives and grid scenarios. Production route three provides a fully off-grid or behind-the-meter scenario with a parametrically optimized mix of wind, solar, and battery storage providing the electricity to produce hydrogen.

Because this study assumes that conventional DRI and Haber-Bosch processes with limited operational flexibility would be employed for steel and ammonia production, respectively, production route three requires large amounts of hydrogen storage to be able to mitigate the intermittency of the wind and solar resources used to produce the hydrogen. The literature has shown that storage in geologic formations, such as salt dome caverns or hard-rock formations, provided they are amenable to hydrogen storage, can achieve much lower storage capital costs than storage in above-ground pressure vessels or buried pipes used as pressure vessels⁴⁹ or cryogenic liquid storage, which is often characterized by high costs and hydrogen losses.^{50,51} Depending on the seasonality of the renewable resources in a given location, the required storage duration could span from tens to hundreds of hours, meaning that locations with both excellent renewable resources and access to geologic storage are highly desirable for low-cost hydrogen production and storage. Both salt caverns and hard-rock formations exist in the US; however, they are not available everywhere. For this reason, we consider locations both with and without access to nearby geologic storage. It is also probable that some amount of hydrogen transport will be necessary even in locations with access to geologic storage unless the electrolyzer, storage well head, and end process can all be located within the same facility. Previous studies have shown that pipeline transport is the most efficient and economic for transferring hydrogen in the quantities expected for industrial processes,^{52,53} and more than 1,600 miles of hydrogen transmission pipeline currently exist in the US.⁵⁴ In this study, we assume that 50 km of pipeline transport will be needed unless specified otherwise, and we pull hydrogen pipeline and compressor capital costs, fixed operating costs, and energy consumption from Argonne National Laboratory's Hydrogen Delivery Scenario Analysis Model (HDSAM) V4.1.⁵⁵ These pipelines are considered only for transport and not for buffer storage.

Candidate locations for renewable-driven steel and ammonia production

The lowest-cost locations for renewable-driven steel and ammonia production are those with excellent renewable resources, access to geologic hydrogen storage, access to low-cost non-hydrogen feedstocks such as iron ore, and access to infrastructure for the distribution of the final product. Figure 2 shows a map of the contiguous US illustrating combined solar- and wind-driven hydrogen production potential, water scarcity, and geologic hydrogen storage. Potential hydrogen demand for ammonia and metals production is located in the Midwest and South regions,^{11,56–58} which could indicate potential hydrogen demand locations. For instance, Minnesota and Indiana are home to iron ore production and large steel plants, respectively,^{56–59} and a large ammonia pipeline crosses parts of Iowa.⁶⁰ West Texas has excellent renewable resources, but it is far from existing steel infrastructure, and parts of it are water constrained (note that some but not all water from hydrogen DRI can be recycled, and detailed assessment of water impacts is beyond the scope of this study). Based on these data, we qualitatively selected five candidate locations—Indiana, West Texas, Iowa, Mississippi, and Minnesota—to represent a diverse com-

bination of the resources, storage, and demand availability. Although none of these locations indicated by red diamonds represent the perfect union between the renewable resource, geologic storage availability, and prevalence of existing infrastructure, each has unique strengths and weaknesses. Table 1 summarizes the benefits and challenges associated with each location. Table S10 provides approximate latitude and longitude and turbine sizes for each location, which we selected taking into account land on which wind farms can be developed based on National Renewable Energy Laboratory (NREL)'s reV model.⁶¹

Mathematical modeling framework

Capturing the performance, economics, and emissions impacts of renewable-driven steel and ammonia production requires techno-economic modeling of wind and solar facilities, electrolyzers, hydrogen storage and transport, and the end-use ammonia and steel production processes. This study integrates several DOE national laboratory tools into a single seamless framework that can perform end-to-end performance, economic, and life-cycle emissions analysis. Figure 3 illustrates the tools used and how information flows between them and through the framework. The framework comprises five modules: renewables and hydrogen systems, hydrogen transport, end use, integrating all pieces, and LCA.

The Hybrid Optimization and Performance Platform (HOPP) model captures the performance and economics of wind and solar plants. The software tool enables detailed analysis and optimization of renewable hybrid power plants down to the component level. Beyond wind (offshore and land-based) and solar plants, it has the capability for the design and analysis of one or combinations of electrical battery storage, geothermal, and hydro.⁶² HOPP also contains a PEM electrolyzer stack model that includes a zero-dimensional cell model that calculates overpotentials as a function of current density^{63–69} and degradation in voltage associated with steady-state operation, dynamic operation, and on-off switching.⁷⁰ Studies have shown that rapid transients and on-off cycling degrade PEM electrolyzers faster than steady-state operation⁶⁹ and have also indicated that safety considerations could limit the turndown ratio of PEM electrolyzers to around 15%.^{71,72} The framework models these operational limits and captures the impact of degradation on overall plant economics. For the off-grid production route, the framework calculates the required hydrogen storage capacity by performing a simple state-of-charge analysis over the course of the year, taking into account the hourly profile of hydrogen coming from the hybrid wind-solar-electrolyzer plant and the flat hydrogen demand profile associated with steelmaking or ammonia synthesis. The model performs parametric optimization to size wind, solar PV, and electrolysis capacities. It parametrically sweeps from no excess wind and solar capacity to 30% excess wind and solar capacity in 10% increments, and for each increment, it also sweeps from a wind-only system design to a solar PV-only system design in 200 MW increments. It then sizes the electrolyzer such that it has adequate capacity to produce the required annual hydrogen for the end-use applications with end-of-life performance (defined as 13% more power than the beginning of life). For this study, we assign battery storage capacity for off-grid systems at 15% of electrolyzer

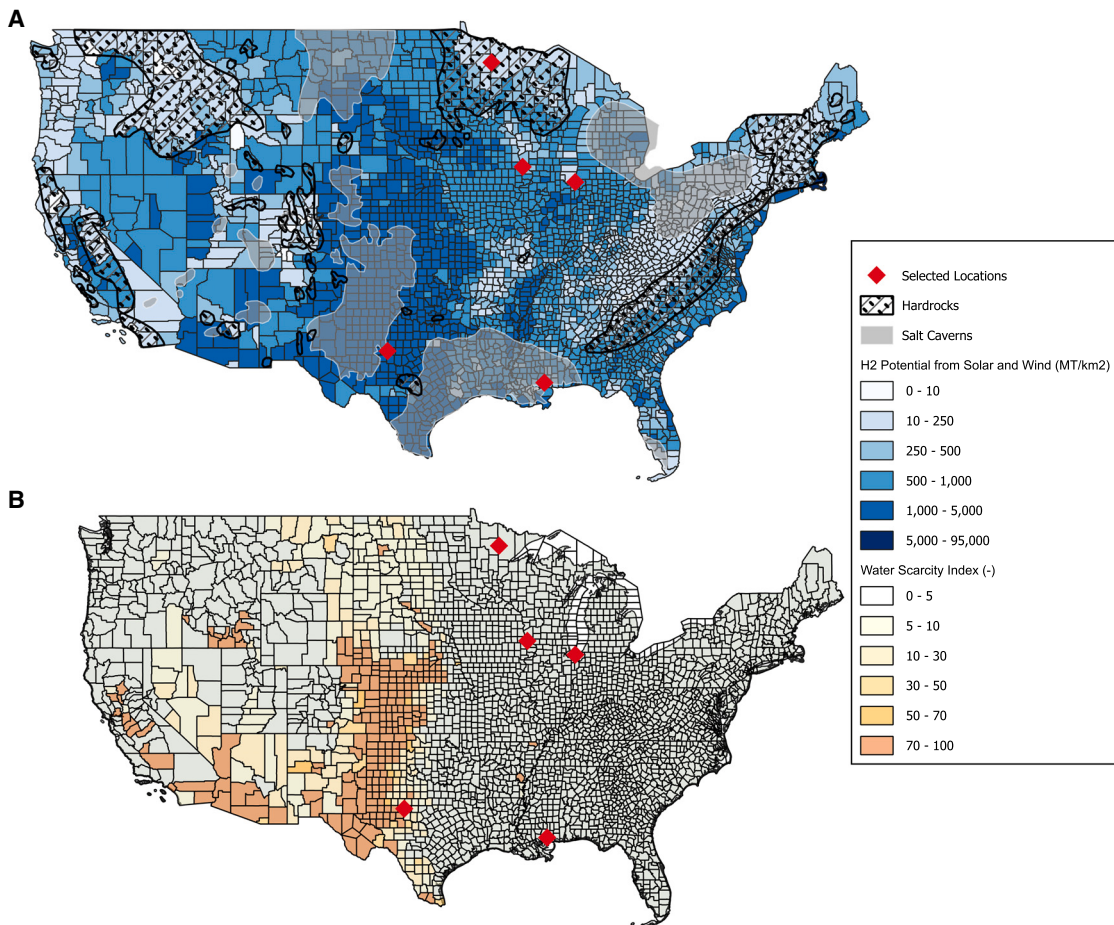


Figure 2. Maps illustrating the locations considered in this study overlaid with renewable resources, geologic storage availability, and water scarcity

(A and B) (A) Renewable resources and hard-rock and salt cavern formations in the US and (B) water scarcity index in the US.

beginning-of-life electrical capacity and 1 h of duration to assist with black starts and handle sub-hourly variations in wind and solar. Previous studies have found that when low-cost hydrogen storage is available, additional battery capacity does not improve the economics of hydrogen production.⁷³ The methods section provides more information on how the model performs system sizing. The grid-connected cases in production route two assume that flat annual retail electricity prices motivated plant owners to operate electrolyzers year-round, and as a result, these scenarios do not require bulk hydrogen storage.

The modeling framework calculates a break-even price or leveled cost of hydrogen (LCOH), leveled cost of steel (LCOS), and leveled cost of ammonia (LCOA) using NREL's Production Financial Analysis Scenario Tool (ProFAST).⁷⁴ ProFAST is a Python-based financial framework based on the core functionalities of H2FAST,⁷⁵ which is a rigorously peer-reviewed financial framework that uses generally accepted accounting principles. Note S1 provides financial parameters used within ProFAST in this study for various technologies to calculate LCOH, LCOS, and LCOA. This study includes potential impacts of current US tax incentives and employs emissions factors from ANL's Green-

house gases, Regulated Emissions, and Energy use in Technologies (GREET) model⁷⁶ to compute scopes 1, 2, and 3 emissions, as defined by the Greenhouse Gas Protocol⁷⁷ for the LCA of the selected production routes and to assess eligibility for tax credits. LCOH is a calculation that represents a revenue stream required to offset all capital, financing, operating costs, and taxation. The IRA has multiple provisions that add tax credit-based cash flow to eligible projects. Such cash flows have no repayment and are strictly reducing the revenue required from sales to cover hydrogen production costs. As such, the revenue requirement for hydrogen production is reduced with any such incentives, and the price of hydrogen can be reduced by the computed amount. The following section provides details on how this study incorporates tax incentives. We use pipeline pipe and compressor capital and operating costs from ANL's HDSAM⁵⁵ along with ProFAST to compute the break-even cost for transporting hydrogen over an assumed distance of 50 km between the points of storage and end use. The framework incorporates capital costs, operating costs, and feedstock consumption for steel and ammonia production derived from process modeling and cost analysis performed

Table 1. Benefits and challenges of candidate locations

| Location | Benefits | Challenges |
|-------------|--|--|
| Indiana | <ul style="list-style-type: none"> existing steel manufacturing low-cost iron ore decent wind resource | <ul style="list-style-type: none"> no geologic storage |
| West Texas | <ul style="list-style-type: none"> excellent wind resource salt cavern storage | <ul style="list-style-type: none"> water-stressed region limited steel distribution infrastructure |
| Iowa | <ul style="list-style-type: none"> close to ammonia and steel demand centers low-cost iron ore good wind resource | <ul style="list-style-type: none"> no geologic storage |
| Mississippi | <ul style="list-style-type: none"> salt cavern storage existing steel and ammonia production | <ul style="list-style-type: none"> poor wind resource |
| Minnesota | <ul style="list-style-type: none"> adequate renewable resource hard-rock formations access to raw materials | <ul style="list-style-type: none"> unknown potential for lined rock caverns |

by Lawrence Berkeley National Laboratory and ANL for steel and ammonia, respectively.^{35,78} In addition to the break-even price of hydrogen and end products, we quantify the life-cycle emissions of hydrogen, steel, and ammonia, and we perform sensitivity analysis on potentially consequential design considerations to demonstrate their impact on costs.

IRA incentives

The IRA provides opportunities for companies to receive various ITCs and PTCs for clean energy technologies, including the electricity PTC (provision 45), the technology-neutral PTC (provision 45Y), the ITC (provision 48), the technology-neutral ITC (provision 48E), the clean hydrogen PTC (provision 45V), and the carbon capture, utilization, and storage credit (provision 45Q).⁷⁹ PTCs specified in provision 45V can be received for 10 years, and those in provision 45Q can be received for 12 years. We compare three incentive scenarios: a “no policy” scenario with no incentives, a “base policy” scenario in which the full 100% credit rates are applied without any additional bonus or credit multipliers, and a “max policy” scenario in which the prevailing wages and apprenticeship utilization requirements are met and domestic content and energy community bonus credits are applied. These scenarios should cover the full range of hydrogen, steel, and ammonia production costs possible when considering incentives. The IRA allows for a taxpayer to stack credits and claim multiple credits for respective components and technologies within one hydrogen production route.⁷⁹ Consequently, most production routes employ credit stacking in the modeling if applicable. Note that the hydrogen PTC cannot be stacked with the carbon capture utilization and storage credit. Table S22 gives further details on credit values and credit stacking.

Eligibility for the hydrogen PTC is based on the well-to-gate emissions intensity of the produced hydrogen, including the scope 1 process emissions (for SMR with CCS; electrolysis has negligible scope 1 process emissions), scope 2 grid power production emissions associated with fuel combustion at fossil fuel-based grid generators, and partial scope 3 emissions accounting for indirect emissions. Note that we do not include technology-embody emissions (e.g., emissions associated with manufacturing wind turbines, solar panels, or electrolyzers)

when assessing IRA 45V eligibility because 45V specifically excludes embodied emissions. We assume that purely off-grid renewable-driven electrolysis production routes are automatically eligible for the full credit. For grid-connected electrolyzers with on-site renewables, we calculate an average annual emissions intensity of the hydrogen produced via both grid electricity and on-site renewables. For grid-only production routes, we calculate the average annual emissions intensity of produced hydrogen solely based on the mix of generators on the grid each year for each location. We use NREL’s Cambium 2022 database⁴³ “Mid-case 100% Decarbonization by 2035” scenario to project what the grid mix will be each year for each location, and we use generator-specific emissions intensity factors from GREET to calculate an average annual hydrogen emissions intensity to use when assessing incentive eligibility, as required by the IRA. The methods section provides more details on LCA calculations, and Note S4 and Tables S23–S25 provide the LCA assumptions used in this study. Because we use grid electricity price and emissions estimates based on a future grid scenario that is consistent with achieving a 100% carbon-free grid nationwide by 2035 (albeit without broad deployment of electrolysis for industrial hydrogen production), the IRA implementation employed in this study should be consistent with the recently finalized US Treasury Department guidance on the implementation of IRA 45V for grid-powered hydrogen production.⁸⁰ Although this grid decarbonization scenario is ambitious, we feel that using this grid scenario provides the best point of comparison to off-grid hydrogen production routes on both cost and emissions bases. We do not include renewable energy credits, energy attribute certificates, or any other method of ensuring a certain grid emissions intensity in this paper, however, because the cost structure of such credits is still uncertain. The following section provides results for LCOH, LCOS, and LCOA, including the range of incentive scenarios varying from receipt of no tax credits to the maximum tax credits achievable. In this regard, we feel that these results capture the full suite of costs achievable with or without incentives.

TEA of hydrogen, steel, and ammonia production

Figure 4 shows the LCOH for all production routes, all locations considered, and for current technology through 2035. The

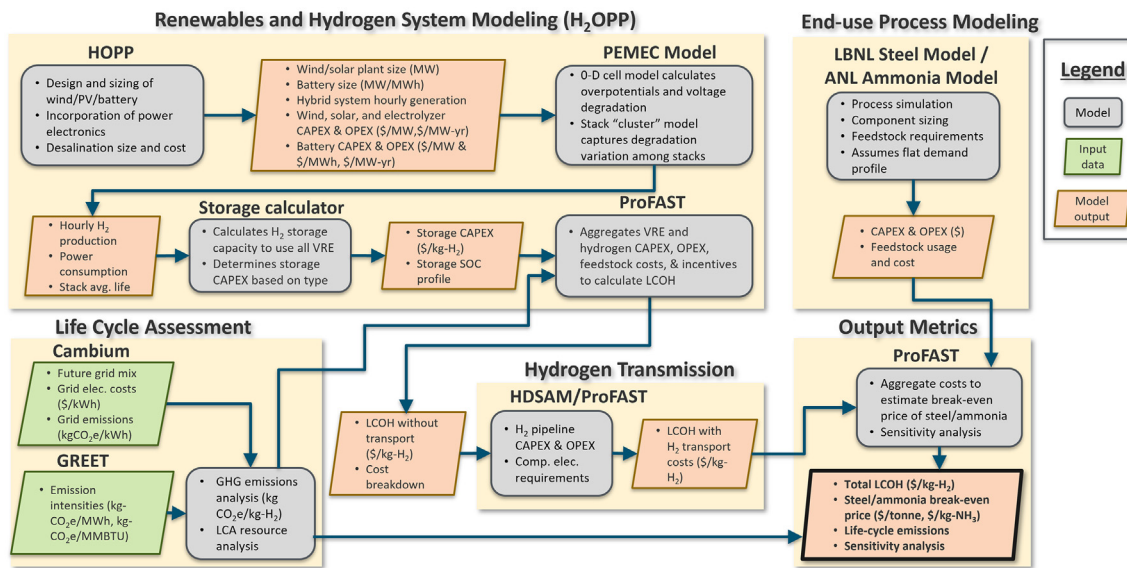


Figure 3. The mathematical model integrates multiple tools into a comprehensive framework for assessing the techno-economics and life-cycle emissions of low-carbon steel and ammonia production

technology year represents the year in which the plant design begins and the vintage of the technology used in a given project. We assume that plant construction starts 2 years later and commissioning occurs 5 years later, corresponding to 2027, 2030, 2035, and 2040 for current technology and technology years 2025, 2030, and 2035 (we assume that “current” technology is that associated with 2022). The error bars represent uncertainty in natural gas prices for the SMR and ATR cases, uncertainty in electrolyzer costs for the electrolysis cases, and uncertainty in grid electricity prices for all grid-connected cases (including SMR, SMR with CCS, and ATR with CCS, which rely on the grid for basic plant operating electricity requirements). The values used for these uncertainties are given in [Figure S3](#) for natural gas prices, [Table S19](#) for electrolyzer prices, and [Table S21](#) for grid prices. The black arrows and dots represent potential savings associated with achieving base IRA tax incentives, and the gray arrows and squares indicate potential savings associated with achieving all feasible IRA tax incentives. [Table S22](#) provides the precise incentives included for different policy scenarios. Projects must commence construction by no later than Jan. 1, 2033, to qualify for the base incentives (meaning that current technology and technology years 2025 and 2030 qualify but technology year 2035 does not), and not all projects will attain the maximum feasible tax incentives. A range of values for the LCOH might therefore be realized, reflecting variations among individual projects.

In the absence of tax incentives, Texas and Minnesota emerge as the most competitive locations for renewable-driven hydrogen production compared with fossil-based routes due to their excellent renewable resources that enable low electricity costs, a relatively high electrolyzer capacity factor, and access to low-cost geologic hydrogen storage. Under baseline assumptions, the off-grid production routes achieve lower costs than grid-only for all years analyzed for all locations because

the cost of electricity from on-site renewables is lower than the estimated retail price of grid electricity. The hybrid on-site renewables and grid production route tends to fall between the grid-only and off-grid production routes for Texas, Mississippi, and Minnesota, while it is occasionally the lowest-cost electrolytic production route in Indiana and Iowa. This occurs because the cost of hydrogen storage is low in Texas, Mississippi, and Minnesota, where geologic storage options exist, but the cost of hydrogen storage is high in Indiana and Iowa, where engineered pressure vessel storage must be deployed. In Indiana and Iowa, the cost of storage outweighs the cost of grid electricity, whereas the opposite is true in the other locations. By 2035, Indiana and Iowa also see lower costs for the off-grid production route than for the hybrid-grid production route. While the off-grid wind + PV + battery production route in Indiana and Iowa is cheaper than the grid-only and hybrid-grid options by 2035, it does not become competitive with fossil-based routes in these locations during any time period considered without incentives. In Minnesota and Texas, the LCOH of off-grid production routes falls within the range of considered assumptions for SMR with CCS and ATR with CCS, making them potentially competitive even without incentives, and in Mississippi this occurs by 2035. The grid-only electrolysis route generally fares worse both with and without incentives due to the high retail prices assumed in this study and the relative difficulty for grid-connected electrolysis to capture IRA tax benefits. The hybrid-grid production route does slightly better, and by 2030, this route in Texas sees LCOH values that fall within the range of assumptions considered for SMR and ATR with CCS. For detailed breakdowns of LCOH in each year and for each electrolysis production route, refer to [Figures S4–S6](#) Indiana, Texas, Iowa, and Minnesota.

[Figure 4](#) illustrates that the IRA incentives have the potential to dramatically reduce LCOH for the off-grid production route. With

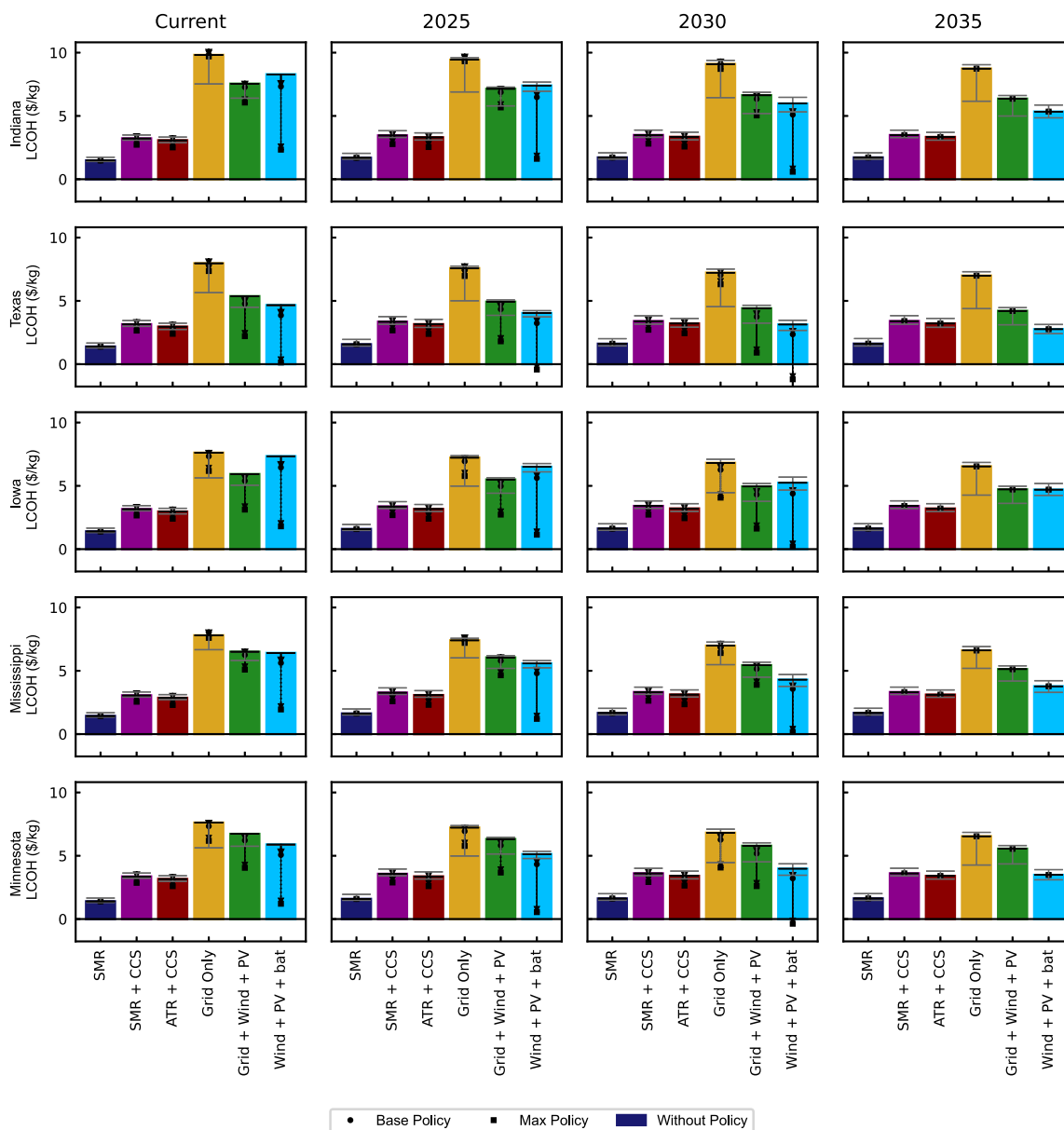


Figure 4. LCOH for all production routes across all locations for current technology through 2035

“Without policy” scenarios have no incentives, base policy scenarios apply the full 100% credit rates without any additional bonus or credit multipliers, and max policy scenarios apply the full 100% credit rates with the prevailing wages and apprenticeship utilization requirements being met and domestic content and energy community bonus credit being applied. The error bars represent uncertainty in natural gas and electricity prices for the SMR cases, uncertainty in electrolyzer costs for the electrolysis cases, and uncertainty in electrolyzer costs and grid electricity prices for all grid-connected cases. Systems that are deployed using equipment from technology year 2035 do not receive incentives because projects that begin construction after January 1, 2033, are not eligible for IRA incentives.

maximum incentives, every location sees this hydrogen production method achieve an LCOH that is competitive with SMR or ATR with CCS with current (2022) technology costs, and the competitiveness of the off-grid production route only increases through technology year 2030. The hybrid-grid production route can also be competitive with SMR or ATR with CCS routes with current technology or in the near future for Texas, Iowa, and Minnesota. Incentives do not benefit the grid-only production route

nearly as much because this production route struggles to achieve low enough annual average emissions to receive tax credits. By technology year 2025, Texas can achieve a negative LCOH with max incentives for the off-grid wind + PV + battery production route, and Minnesota follows suit in 2030. In the context of this study, a negative LCOH means that the price that plant owners would need to charge to achieve their desired rate of return is negative if they are able to take full advantage of

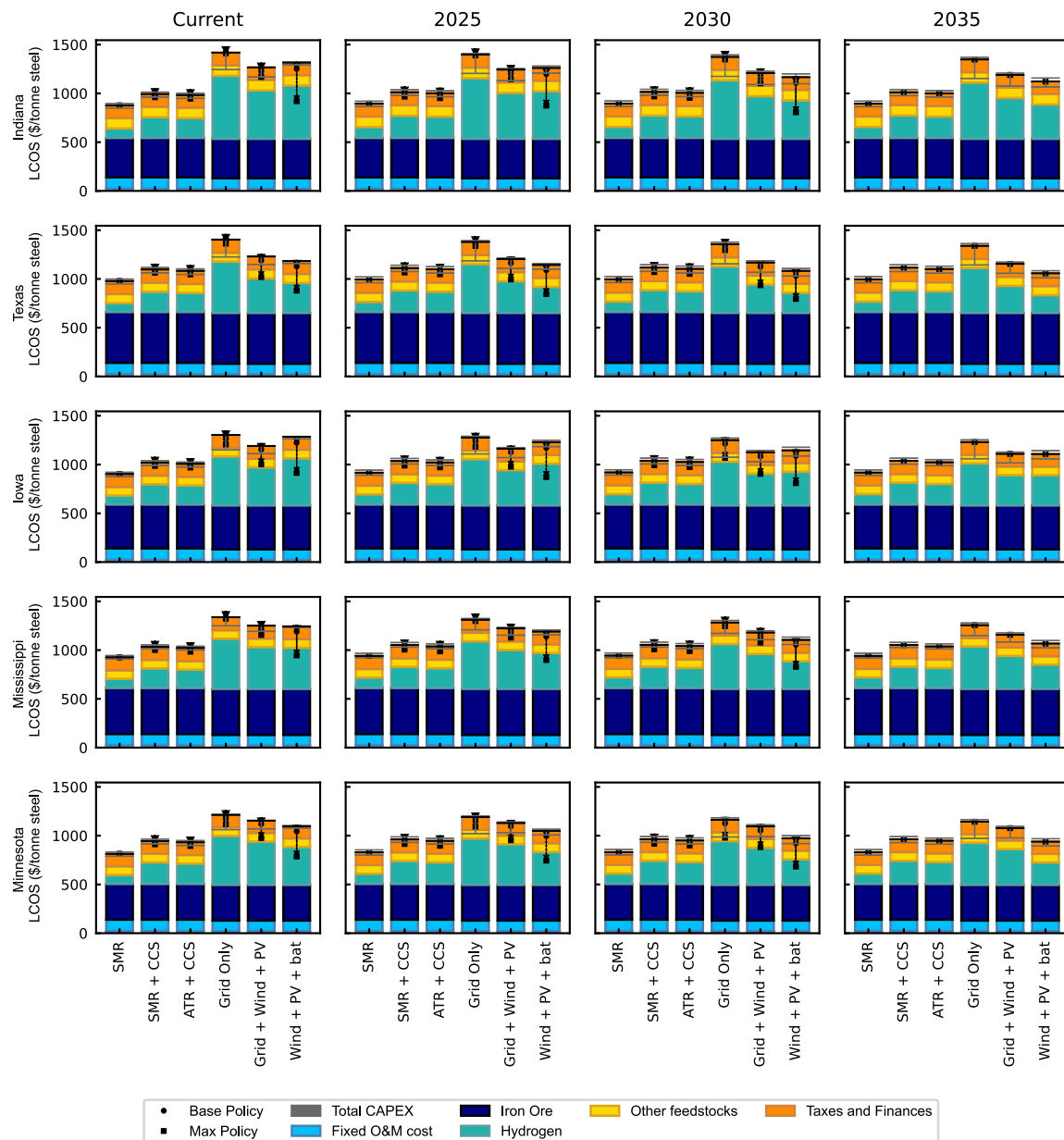


Figure 5. LCOS for all production routes across all locations for current technology through technology year 2035

Bar totals correspond to no incentives. Base policy scenarios apply the full 100% credit rates without any additional bonus or credit multipliers, and max policy scenarios apply the full 100% credit rates with the prevailing wages and apprenticeship utilization requirements being met and domestic content and energy community bonus credit being applied. The error bars represent uncertainty in natural gas and electricity prices for the SMR cases, uncertainty in electrolyzer costs for the electrolysis cases, and uncertainty in electrolyzer costs and grid electricity prices for all grid-connected cases. “Other feedstocks” include maintenance materials, water, lime, carbon, natural gas, electricity, and slag disposal. Systems that are deployed using equipment from technology year 2035 do not receive incentives because projects that begin construction after January 1, 2033, are not eligible for IRA incentives.

IRA incentives. In practice, hydrogen production plant owners are unlikely to charge negative prices for hydrogen and would instead enjoy a higher rate of return than that assumed in this study. Because this study focuses on determining the potential costs of steel and ammonia production with hydrogen as a feedstock, however, we assume that all scenarios aim for the same rate of return given in Table S1.

Figure 5 shows the levelized cost or break-even price of virgin steel production using DRI-EAF for all hydrogen production routes across all locations for current technology through 2035. Like Figure 4, the error bars in Figure 5 represent uncertainty in natural gas prices for the SMR cases, uncertainty in electrolyzer costs for the electrolysis cases, and uncertainty in grid electricity prices for all grid-connected cases, while the black arrows and

dots represent potential savings associated with achieving base IRA tax incentives, and the gray arrows and squares indicate potential savings associated with achieving all feasible IRA tax incentives. Note that fixed operations and maintenance costs, iron ore feedstock, and other feedstock costs comprise a significant portion of the break-even price of steel. While total CAPEX, fixed O&M, and “other feedstock” costs are more or less constant across all locations, the cost of iron ore mining and delivery can vary substantially across locations primarily due to the feedstock transportation to the steelmaking site. Consequently, locations with the lowest hydrogen production costs might not necessarily achieve the lowest cost of steel.

Nonetheless, all locations can achieve steel production costs competitive with SMR without CCS in that same location by employing the off-grid electrolysis-based hydrogen production route with current technology costs when reaping the maximum benefits of IRA incentives. In technology year 2025, maximum IRA incentives enable the off-grid wind + PV + battery production route to achieve lower LCOS than SMR without CCS in every location, and they enable the hybrid-grid production route to fall within the range of uncertainty of this study’s assumptions for ATR with CCS in all locations except for Indiana by technology year 2030. In the absence of incentives in technology year 2035, Texas, Iowa, Mississippi, and Minnesota each see the off-grid electrolysis-based production route achieve a LCOS that overlaps with SMR and ATR with CCS when considering the full range of assumptions. The subsequent section details the regional sensitivity of steel production costs in greater depth.

Figure 6 shows the LCOA production for all production routes across all locations for current technology through technology year 2035. Once again, the error bars in Figure 6 represent uncertainty in natural gas prices for the SMR cases, uncertainty in electrolyzer costs for the electrolysis cases, and uncertainty in grid electricity prices for all grid-connected cases, while the black arrows and dots represent potential savings associated with achieving base IRA tax incentives, and the gray arrows and squares indicate potential savings associated with achieving all feasible IRA tax incentives. Because ammonia production costs are primarily driven by hydrogen production costs for all production routes, these results closely resemble those for hydrogen production costs. Specifically, all locations see the off-grid electrolysis-based route as highly competitive with SMR and ATR with CCS with current technology and maximum incentives, with the off-grid wind + PV + battery case in Texas achieving a negative break-even price of ammonia by 2030 with maximum incentives. Texas and Minnesota both see the off-grid wind + PV + battery production route directly compete with SMR and ATR with CCS in 2035 in the absence of incentives.

Regional sensitivity analysis of steel production costs

Figure 7 shows a regional sensitivity analysis of the break-even price of steel for all production routes across all incentive scenarios for current technology through 2035, which is a slightly different way to visualize the data presented in Figure 5. With no incentives or base incentives, SMR without CCS in Minnesota achieves the lowest break-even prices of any production route, location, or year, followed by ATR with CCS and SMR with CCS. By technology year 2035, however, the off-grid wind +

PV + battery production route is competitive with ATR and SMR with CCS in Minnesota. With maximum incentive utilization in 2030, the off-grid electrolysis production route in all locations achieves lower steel production costs than SMR in Minnesota. Maximum incentives also enable the off-grid production route in all locations to be competitive with the SMR and ATR with CCS routes in 2025, while the off-grid production route in Minnesota achieves lower cost than the SMR production route in Minnesota with current costs and maximum incentives. Note that no results are shown for base and max incentives for technology year 2035 because this timeframe correspond to plant construction commencing in 2037 or later, which is after the deadline for plants to begin construction and receive any IRA incentives.

Despite having the lowest hydrogen production cost, Texas does not achieve the lowest break-even cost for steel. This is because of the high cost to transport iron ore to Texas, which we estimate at approximately \$96/ton steel for transportation, compared with the range of approximately \$0.7–\$66/ton steel for transportation to the other locations (the *methods* section provides more information on feedstock transport cost estimation). This illustrates the importance of both low hydrogen costs and proximity to low-cost iron ore in achieving low steel production costs via electrolytic hydrogen production.

The value of hybrid wind-solar systems

Table 2 provides the parametrically optimized design results for the off-grid and hybrid-grid electrolysis production routes for 2030 with no incentives. Results deviate slightly based on technology year and policy level but generally fall close to the values given in this table. For the off-grid production route, we parametrically swept from no excess renewable capacity to 30% excess renewable capacity, and for each excess renewable energy step, we swept from pure wind generation to pure solar generation in 200 MW-AC capacity steps. For the hybrid-grid production route, we swept from zero renewable energy capacity to 500 MW of renewable energy capacity in 100 MW increments, and for each step, swept from pure wind generation to pure solar generation in 50 MW increments. Note that wind-rated capacity does not correlate to the precise renewable capacity step because the wind plant is sized so that its maximum output matches the renewable capacity step, and as modeled in PySAM, the maximum wind plant output is approximately 81% of rated capacity.

For the off-grid production route, all locations see several hundred megawatts of both wind and solar capacity and benefit from installing 10% more electricity generation capacity than would be strictly required to produce the hydrogen required by the end-use applications. This occurs because renewables are relatively inexpensive compared with the electrolyzer and hydrogen storage, and installing excess renewables enables the electrolyzer to operate with a higher capacity factor and a smoother annual operating profile. These qualities reduce the required storage capacity and reduce the impact of electrolyzer and hydrogen storage capital costs on LCOH. For the sake of completeness, we have included battery power capacity and duration, but note that these values are fixed at 15% of electrolyzer capacity and 1 h of duration to assist with black starts and sub-hourly variations in wind and/or solar generation. For the hybrid-grid production route, every location installs the

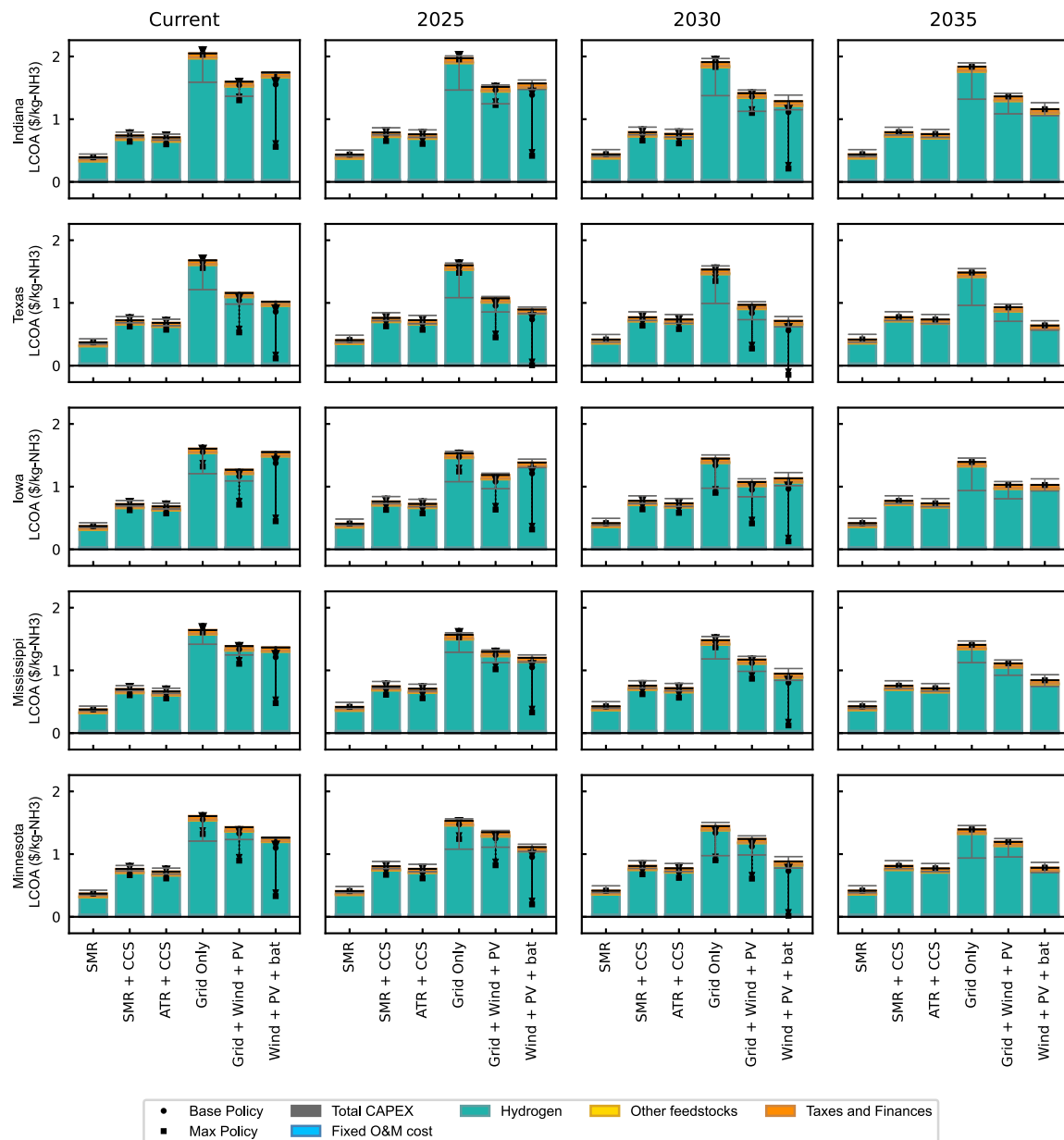


Figure 6. LCOA for all production routes across all locations for current technology through technology year 2035

Bar totals correspond to no incentives. Base policy scenarios apply the full 100% credit rates without any additional bonus or credit multipliers, and max policy scenarios apply the full 100% credit rates with the prevailing wages and apprenticeship utilization requirements being met and domestic content and energy community bonus credit being applied. The error bars represent uncertainty in natural gas and electricity prices for the SMR cases, uncertainty in electrolyzer costs for the electrolysis cases, and uncertainty in electrolyzer costs and grid electricity prices for all grid-connected cases. Other feedstocks include electricity, cooling water, and the iron-based catalyst. Systems that are deployed using equipment from technology year 2035 do not receive incentives because projects that begin construction after January 1, 2033, are not eligible for IRA incentives.

maximum amount of wind energy such that the wind plant can fully power the electrolyzer at peak generation. None of the locations install any solar PV for the hybrid-grid production route. This occurs because the primary benefit of solar PV is to enable higher electrolyzer capacity factor and a smoother electrolyzer operating profile. In a grid-connected system, the grid already provides these services at lower cost.

LCA of hydrogen, steel, and ammonia production routes

Figure 8 shows the hydrogen production life-cycle emissions for all production routes across all locations for current technology through 2035. Here, we include infrastructure or “embedded” emissions in our analysis to fully capture the expected emissions impact of each production route, and this defers from the emissions included when assessing IRA 45V eligibility, which does

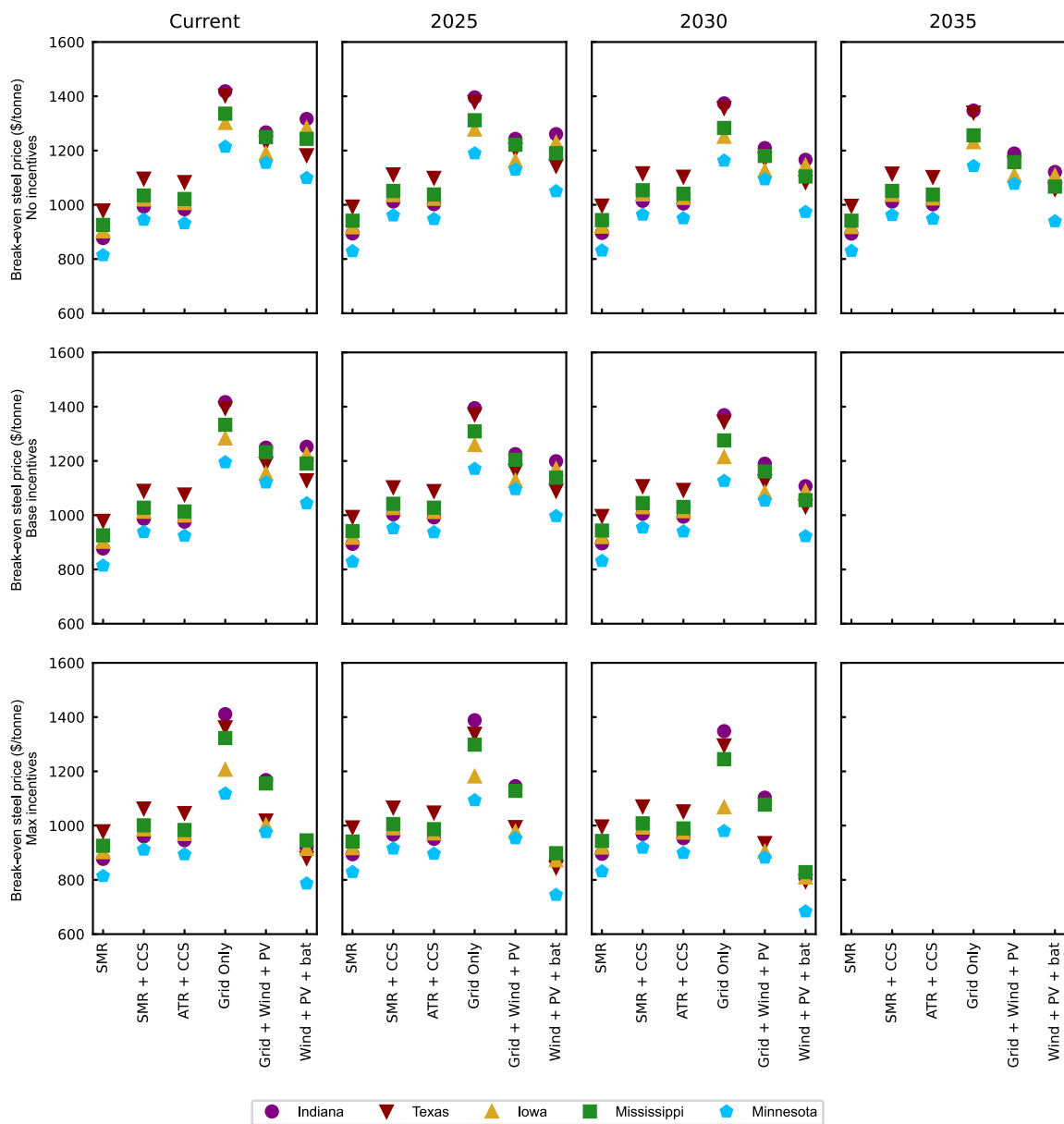


Figure 7. Regional sensitivity of LCOS for all production routes across all incentive scenarios for current technology through technology year 2035

No results are shown for base and max incentives for technology year 2035 because this time frame corresponds to plant construction commencing in 2037 or later, which is after the deadline for plants to begin construction and receive any IRA incentives.

not require inclusion of embedded emissions. We also use long-run marginal emission rates for grid-related emissions rather than the average annual emissions that are required for assessment of IRA 45V eligibility. We make this distinction because long-run marginal emission rates better reflect the actual emissions associated with the new electrolysis capacity, but it is not actually possible or practical to quantify these emissions for tax credit eligibility assessment; hence, the IRA requires average annual emissions.

SMR and ATR with CCS and all electrolysis-based hydrogen production methods achieve much lower life-cycle emissions

than SMR, which has scope 1 emissions associated with the direct production of CO₂ and scope 3 emissions associated with natural gas recovery. The SMR and ATR with CCS production routes incur a small amount of scope 1 emissions associated with incomplete carbon capture. For technology year 2025, all grid-connected electrolysis cases incur a small amount of scope 2 emissions associated with grid electricity generation emissions. Recall that technology year 2025 corresponds to a plant commissioning date 5 years later, in 2030. Under the assumption that the grid follows NREL's 100% decarbonization by 2035 standard scenario, the energy from the grid has only non-zero

Table 2. Off-grid and hybrid-grid plant design results for technology year 2030 with no incentives

| Parameter | Indiana | Texas | Iowa | Mississippi | Minnesota |
|--|---------|-------|-------|-------------|-----------|
| Off-grid production route | | | | | |
| Optimal excess wind/solar annual generation (%) | 10 | 10 | 10 | 10 | 10 |
| Optimal wind farm capacity (MW) | 690 | 888 | 722 | 888 | 930 |
| Optimal solar PV capacity (MW-AC) | 1200 | 400 | 1,000 | 1,000 | 800 |
| Optimal electrolyzer rated capacity at BOL (MW) ^a | 920 | 640 | 800 | 760 | 720 |
| Battery power capacity (MW) ^b | 138 | 96 | 120 | 114 | 108 |
| Battery storage duration (h) ^c | 1 | 1 | 1 | 1 | 1 |
| Electrolyzer capacity factor (%) | 53% | 73% | 60% | 63% | 66% |
| Average electrolyzer stack life (years) | 5.04 | 6.31 | 5.52 | 5.02 | 5.55 |
| Hydrogen storage capacity (tons) | 1,758 | 3,282 | 1,339 | 4,927 | 1,566 |
| Hybrid-grid production route | | | | | |
| Optimal wind farm capacity (MW) | 618 | 618 | 631 | 618 | 618 |
| Optimal solar PV capacity (MW-AC) | 0 | 0 | 0 | 0 | 0 |
| Electrolyzer rated capacity at BOL (MW) ^d | 480 | 480 | 480 | 480 | 480 |
| Electrolyzer capacity factor (%) ^d | 95% | 95% | 95% | 95% | 95% |
| Average electrolyzer stack life (years) | 8.91 | 8.91 | 8.91 | 8.91 | 8.91 |
| Hydrogen storage capacity (tons) | 0 | 0 | 0 | 0 | 0 |

^aEnd of life defined by 13% increase in voltage/power at a rated H₂ production rate.

^bBattery capacity fixed at 15% of the electrolyzer electrical capacity.

^cBattery storage duration fixed at 1 h.

^dElectrolyzer capacity for hybrid-grid fixed at 480 MW with capacity factor of 95%.

emissions (scopes 1 and 2) between 2030 and 2034. As a result, technology years 2030 and 2035, which correspond to commissioning dates of 2035 and 2040, do not have any scope 2 emissions. All hydrogen production routes have scope 3 emissions corresponding to their respective supply chains, including embedded infrastructure emissions associated with wind turbines, solar panels, different types of power generators contributing to the grid (nuclear, hydro, etc.), and electrolyzers, where applicable. For electrolysis production routes, we quantify scope 3 emissions based on the proportion of energy delivered from each electricity production source within the Cambium scenario and the scope 3 emissions associated with each power source and feedstock according to the GREET model.⁷⁶ Interestingly, off-grid production routes tend to have slightly higher scope 3 and overall emissions than grid-connected production routes. This is likely due to off-grid routes having higher solar PV capacity, leading to higher indirect emissions associated with material extraction and panel manufacturing. This is somewhat ironic considering that off-grid systems can obtain much more significant IRA 45V PTCs than grid-connected systems due to IRA 45V's reliance on annual average emissions without scope 3 emissions for incentive eligibility assessment. It is important to emphasize, however, that the difference between grid-only and off-grid emissions is quite small, and both production routes achieve low emissions in this analysis. The grid-only production route emissions will also be much higher if the 100% Decarbonization by 2035 Cambium scenario is not realized in practice.

Figures S7 and S8 show steel and ammonia life-cycle emissions, respectively, for all production routes across all loca-

tions for current technology through 2035. The different production routes generally follow the same trends as those seen for hydrogen production-related emissions. The steel process also incurs indirect emissions from the extraction and processing of lime, iron ore, and the small amount of natural gas that supplements hydrogen for steelmaking. The steel process also incurs scope 3 indirect emissions from the extraction and processing of lime, iron ore, and the small amount of natural gas that supplements hydrogen for steelmaking. The ammonia production scope 3 emissions essentially depend on the hydrogen GHG emissions because this is the only feedstock that is produced upstream of the NH₃ plant, and emissions associated with N₂ separation are considered at the ammonia plant level and work out as scope 2 emissions associated with grid electricity used to power the air separator.

DISCUSSION

This analysis demonstrates that hybrid off-grid renewable energy-powered electrolysis plants could potentially be cost competitive with hydrogen production via SMR with or without CCS and ATR with CCS for both ammonia production and steel production via DRI. This holds true with adequate utilization of IRA incentives and, in some cases, even in the absence of incentives. Several key criteria must be met for these plants to achieve cost competitiveness. This section discusses these criteria along with general insights elucidated by this study and several caveats that should be considered.

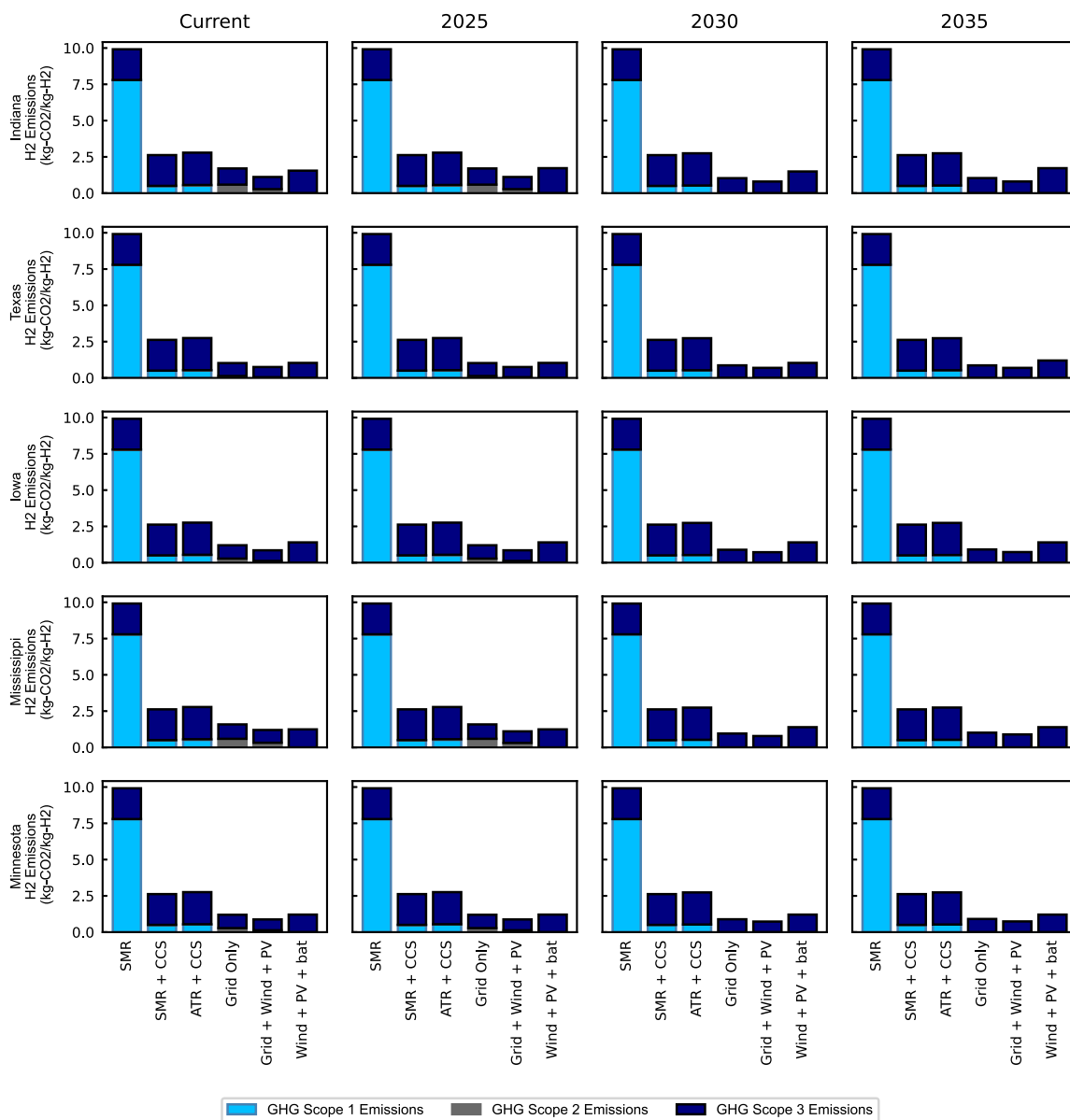


Figure 8. Life-cycle emissions of hydrogen production for all production routes across all locations for current technology through 2035

A key requirement for electrolytic hydrogen production to compete with SMR in industrial applications is that the total hydrogen system storage and transport costs must be low. Ideally, the selected location would have both ample renewable resources and available geologic hydrogen storage. Hydrogen transport does not significantly contribute to delivered hydrogen costs at the distance assumed in this study (50 km). In practice, this distance could vary for different projects, and multiple potential producers might compete to demonstrate the lowest delivered cost of hydrogen. In these scenarios, transport cost might influence which producer wins a purchase agreement. The transport of hydrogen over longer distances might be economically feasible if the production and storage costs are

low enough. Because this study focuses on co-located systems, analysis of the buildup of hydrogen networks allowing for the transport of cheap hydrogen from remote locations is outside the scope.

If a project must use pressure vessel storage due to a lack of access to cheap storage options, it might benefit from implementing technologies to improve the flexibility of the end-use processes so that steel or ammonia production can be more tolerant of the intermittency of renewable generation and require less storage capacity. Steel production could use intermittent batch operation of the DRI using the MIDREX Flex technology⁸¹ to increase flexibility, and ammonia production could use catalysts suitable for low temperature and pressure operation and

advanced process control.^{82–85} Note that these methods and technologies require further analysis and testing to be fully vetted as viable. Additionally, the use of pressure vessels at large scales might not be sensible due to the land footprint and the sheer amount of steel required. New hydrogen storage technologies that can be located without geologic requirements, such as liquid organic hydrogen carriers, could substantially broaden the regions in which electrolytic hydrogen production is cost competitive for industrial applications if material-based storage can achieve low enough costs.³⁵

The steel plant location selection is also very important because delivered iron ore costs comprise a significant portion of steel production costs. In most cases, the delivered iron ore costs contribute more than the cost of hydrogen. For this reason, producing steel using renewable-driven electrolytic hydrogen benefits from being located in close proximity to sources of low-cost iron ore. The cost of ammonia is primarily driven by the cost of hydrogen, so ammonia production siting is less sensitive to proximity to non-hydrogen feedstocks. Note that all technologies considered in this study can have impacts on local communities, and community engagement is a key consideration regardless of production route. Proximity to and availability of markets and transportation of steel and ammonia are also important considerations that are outside the scope of this work.

Colocating and over-sizing complementary wind and solar PV for electrolytic hydrogen production has the potential to reduce the LCOH in locations with limited wind resources and a shortage of low-cost hydrogen storage by providing a steadier supply of electricity. This increases the capacity factor of the electrolyzer, reduces the amount of required storage, and lessens both ramp rates and on-off cycling of the electrolyzer stacks. Enabling a steadier electrolyzer operating profile leads to less electrolyzer degradation and a longer electrolyzer stack life. All these impacts help to reduce LCOH.

A final key insight is that in technology year 2035, after incentives have expired, the off-grid electrolysis-based production route achieves hydrogen cost competitiveness with SMR or ATR with CCS in Texas and Minnesota. Depending on the uncertainty in electrolyzer and natural gas prices, however, electrolysis-driven production routes might come close to being cost competitive for these applications in 2035 in Mississippi as well. The off-grid electrolysis-based production route achieves steel cost competitiveness with SMR or ATR with CCS in Minnesota but is less competitive in other locations due to the higher cost of transporting iron ore to the locations. The fossil-based production route costs are highly sensitive to natural gas prices, and this study uses future gas price projections for the US from the US Energy Information Administration (EIA) Annual Energy Outlook (AEO)⁸⁶ that range between \$3/MMBTU in Texas in 2030 to \$6.7/MMBTU in Indiana in 2041. If natural gas prices end up higher than these projections, then more electrolysis production routes might be economically competitive without incentives. Similarly, regions outside the US with higher natural gas prices but similar renewable costs, renewable resources, and geologic storage availability could see renewable-driven electrolysis production routes that are competitive with fossil fuel-based production routes. The final regulations for IRA 45V⁸⁰ could also motivate hydrogen producers to withdraw electricity

from the grid in an intermittent fashion in locations that do not meet the Treasury Department's definition for low-emission grid electricity. These considerations are outside the scope of the current analysis but constitute important fields of research.

Limitations of the study

An important caveat of this study is that the results heavily depend on the assumed financial parameters, from which reality could significantly deviate. Future grid electricity retail prices are also highly uncertain. Previous studies have compared grid-connected and off-grid electrolysis economics and concluded that grid connectivity reduces hydrogen production costs relative to off-grid electrolysis systems largely by increasing the electrolyzer capacity factor and/or achieving lower total electricity costs.^{87–89} Conclusions of this nature depend on a number of assumptions within these models that differ from those used in the present analysis. For example, Eichman et al.⁸⁷ and Koleva et al.⁸⁸ consider solar PV only for their off-grid cases. Solar PV-only systems tend to have much lower capacity factors than wind-only or wind and PV hybrid systems, resulting in higher LCOH due to low electrolyzer utilization. Guerra, Eichman, Hurlbut, and Xu⁸⁹ optimize hybrid wind, PV, and grid-connected electrolysis systems and find that all scenarios considered rely on the grid to some extent; however, they also assume pressure vessel storage, which is much more expensive than geologic hydrogen storage. These studies also assume higher electrolyzer capital costs than this study, which causes annual electrolyzer utilization to have a larger impact on LCOH. It is important to recognize that the low-cost off-grid hydrogen production routes portrayed in this study have relatively high capacity factors due to complementary wind and solar resources, low geologic hydrogen storage costs where salt caverns or hard-rock cavern development is feasible, and low electrolyzer costs relative to the previously mentioned studies. All these attributes contribute to off-grid systems achieving more competitive hydrogen production costs. Our analysis also estimates higher retail electricity rates than previous analyses because it incorporates costs associated with decarbonizing the electric grid. We employ capacity expansion and production cost modeling results to estimate future wholesale prices⁴³ and baseline these against AEO data for current retail prices,⁸⁶ as discussed in the *methods* section, and the results indicate that all locations considered could potentially achieve lower LCOS with the off-grid electrolysis production routes than with the grid-only electrolysis production route. This finding is consistent with that from Devlin et al.,³ who compare islanded (off-grid) electrolytic hydrogen for DRI-EAF with both grid-powered hydrogen production and conventional BF steel production for plants co-located with a number of iron ore deposits around the world. They employ current industrial electricity tariffs in conjunction with projected grid carbon intensities and find that several countries, including the US, could see lower steel production costs via off-grid systems than with grid-powered electrolysis. Nonetheless, estimating future retail rates is inherently difficult because retail prices are typically established through rate-making processes that seek to balance cost recovery, equity, and cost causation,⁴³ each of which can be specific to individual utilities. Time-of-use (TOU) or real-time pricing (RTP) structures could potentially be more

beneficial than annually fixed rates for industrial electricity consumers for the aggressive grid decarbonization scenario used in this study, particularly if those consumers have access to hydrogen storage or can leverage flexible steel and ammonia production processes. Assessing TOU or RTP structures would require a detailed analysis of how those structures might relate to wholesale marginal electricity costs, dispatch optimization to identify how these structures would impact electrolyzer plant operation, and ideally some accounting for how GW-scale electrolyzers might in turn impact grid electricity costs. Most analyses that use hourly varying RTP structures still use the same price-taker assumption employed in this study, and in the future, this assumption should be better assessed because recent studies have found that it can be inaccurate for modern electricity grids with moderate renewable penetration.⁹⁰ These tasks are outside the scope of the present analysis but will be important for more comprehensive analyses of future decarbonized grid operation and its impact on the economics of grid-powered electrolysis.

Another important caveat of this study is that we have employed general correlations for salt cavern and lined rock cavern storage costs and studied general maps of where these formations lie. The precise geologic storage costs in individual locations could vary significantly from these estimates depending on local conditions. The same is true for carbon sequestration. Although this study uses region-specific CCS costs,⁹¹ real-world costs could deviate from these assumptions, resulting in discrepancies relative to the results presented herein. AEL or solid oxide electrolyzers could also be employed in place of PEM electrolyzers, though each comes with its own challenges and caveats. Analysis of these types of electrolyzers is beyond the scope of the present analysis but a worthy topic for future research.

This study also employs a parametric optimization approach to size wind, solar PV, and electrolyzer plant capacities. Employing mixed-integer linear programming to optimize the sizing of these subsystems might result in configurations that achieve lower LCOH, but this would require significant simplifications to the mathematics of electrolyzer degradation. For this study, we prioritized fidelity in renewable plant and electrolyzer modeling, including electrolyzer stack degradation, over subsystem capacity optimization. PEM electrolyzer degradation is still being investigated, however, and the impacts of dynamic operation on life are not completely understood. There are also many external factors that could impact the feasibility and cost of renewable-driven electrolytic hydrogen production for steel and ammonia plants in different locations, such as zoning laws, permitting times, local acceptance of the technologies, and risk tolerance of the institutions that might finance these projects. There is also uncertainty about which applications will gain access to the best renewable resource locations first. We have also only considered five locations in this study. A more thorough geospatial analysis is necessary to identify all the best locations and determine how much steel and/or ammonia production can be decarbonized using renewable-driven electrolytic hydrogen production.

Finally, we emphasize that this analysis focuses on hydrogen production for industrial applications within the contiguous US. Other regions of the world, such as Europe, face higher natural

gas prices, while others have better wind and solar resources. The results of this study should thus be considered applicable to the specific regions within the US that were assessed and not extrapolated to other regions or other parts of the world.

METHODS

DRI steel production process modeling

Capital, operating, and feedstock costs, along with feedstock consumption, were extracted from the process modeling of the DRI process³⁵ in the process simulation software ProSimPlus.⁹² The model's boundary consists of the DRI steel mill, EAF, off-gas treatment, heat and electricity demand for ladle refining operations, and a cooling water system. Fuels, chemicals, and feedstocks—such as electricity, natural gas, carbon, lime, and iron ore pellets—are assumed to be procured at their delivered prices to the plant. The costs and feedstock requirements for the DRI process are based on an iron ore pellet composition of 95 wt % Fe₂O₃, 2 wt % Al₂O₃, 3 wt % SiO₂.³⁵ This composition corresponds to approximately 66% Fe, which is within the desired range of Fe content for the DRI process. A detailed description of the simulation model can be found in the literature.³⁵ Figure S1 illustrates a simplified flowchart of the simulated process, which was modeled at a capacity of 1 MMT of steel per year.

We derived correlations of the various plant component capital costs as a function of the annual steel slab production capacity using results from the process simulation. Table S2 summarizes the steel plant component costs,³⁵ Table S3 summarizes the steel plant feedstock consumption and costs and the by-product production and disposal costs,³⁵ and Table S4 summarizes the steel plant feedstock transportation costs compiled using a custom commodity transport cost model that uses Bureau of Transportation Statistics.⁹³ Note that the steelmaking process itself requires approximately 0.55 MWh of electricity per metric ton of annual steel slab produced,³⁵ which we assume comes from the grid regardless of the production route. Further, roughly 0.72 GJ-LHV of natural gas per metric ton of annual steel slab is used as a makeup gas to hydrogen to meet the total heat load and as a source of carbon in the steel.³⁵ This means that hydrogen does not replace 100% of the natural gas in the modeled process, which is reflected in Figure S7.

Haber-Bosch ammonia production process modeling

We developed correlations for capital costs for ammonia production via Haber-Bosch using a process model developed in Aspen Plus and comprehensively described in Lee et al.⁷⁸ Figure S2 presents the simulated system, including the Haber-Bosch loop, the boiler and steam turbine system, the cryogenic distillation air separation system for nitrogen extraction, and a cooling tower. The reactor was modeled as four plug flow reactors with intercooling to maintain reactor temperatures between 300°C and 500°C.

We used the scaling laws from Lee et al.,⁷⁸ outlined in Note S2, to calculate the direct capital, fixed operations and maintenance, and variable operations and maintenance costs as a function of the plant design capacity. The correlations' constants and scaling factors are shown in Table S5, and Table S6 gives feedstock and byproduct consumption/production rates and costs,

and interested readers should refer to Lee et al.⁷⁸ for more information on how they modeled the Haber-Bosch process.

SMR plant costing

Table S7 summarizes the major assumptions for SMR plants with and without CCS. The correlations for the capital investment costs are derived using NREL's Hydrogen Analysis (H2A) tool, version Aug. 2022.⁹⁴ Carbon dioxide transportation and sequestration costs for SMR + CCS plants were derived using the Fossil Energy/National Energy Technology Laboratory (FE/NETL) CO₂ Saline Storage Cost⁹¹ and the FE/NETL CO₂ Transport Cost⁹⁵ models. Table S9 lists the transport and storage costs for each location to the closest formation.

Natural gas prices can substantially vary from one year and/or region to another. Figure S3 shows the base, low, and high natural gas cost cases used in this study based on projected regional data acquired from the EIA AEO 2023.⁹⁶ The base case represents the reference case for regional projected industrial natural gas prices, and the low and high cases exemplify the high and low oil and gas supply alternative scenarios from AEO 2023, respectively.

Hybrid renewable-hydrogen system technology sizing

The modeling framework sizes wind plants, solar plants, and electrolyzers to deliver sufficient hydrogen to reduce (i.e., remove oxygen from) iron ore needed by a steel plant that produces approximately 1 MMT of steel per year (which corresponds to approximately 334,000 metric tons of ammonia per year) with a 90% steel plant capacity factor. The total electrolyzer, wind, and solar capacity can vary by grid connectivity scenario and location. Given that the steel production process previously outlined requires approximately 0.07 metric tons of hydrogen to produce 1 metric ton of steel and that the PEM electrolyzer modeled in this study requires 54.6 kWh/kg of hydrogen produced, a grid-connected electrolyzer operating with a 90% capacity factor would require a capacity of 456.8 MW. Because this study assumes 40-MW balance-of-plant modules for the electrolyzer, for reasons described in the next section, we round the total grid-connected electrolyzer capacity to 480 MW. Grid-connected electrolyzers with a fixed annual average electricity rate would operate any time that the steel or ammonia plant operates to minimize the need for storage and the impact of overall capital costs on the production costs of hydrogen, steel, and/or ammonia.

For the grid + wind + solar production route, the model runs a parametric sweep of wind and solar capacities from no renewable capacity to 500 MW of combined capacity in 100 MW increments. For each 100 MW increment, it sweeps from wind-only to solar-only in 50 MW increments. After completing the parametric sweep, the framework selects the combination of wind and solar capacities that provides the lowest LCOH. For the off-grid production route, the model runs a parametric sweep for both the amount of excess renewable generation capacity installed and the amount of wind and solar capacity installed. It starts by sweeping from no excess renewable capacity to 30% excess renewable capacity in 10% increments, where excess is defined as generation capacity beyond what is necessary to produce the annual amount of hydrogen necessary for 1 MMT of steel. For each increment of excess renewable capacity, the mathematical modeling framework sweeps from wind-only to solar-only in 200

MW increments, and for each of those increments, it sizes the electrolyzer to the minimum size such that with end-of-life stack performance, it can produce the required annual amount of hydrogen necessary for 1 MMT of steel. After completing all sweeps, the model chooses the combination of wind, solar PV, and electrolyzer capacities that results in minimum LCOH.

This approach requires a preliminary estimate of wind and solar PV capacity factors for each location to establish the wind-only capacity and the solar-only capacity that bookend the parametric sweep. The individual wind turbines are sized to provide the lowest levelized cost of energy for each region, which is the established practice in the field of wind plant design.⁹⁷

Table S10 displays the approximate capacity factor for the wind and solar plants at each location, along with wind turbine rotor diameter, hub height, and total power rating. The modeling framework uses PySAM⁹⁸ to obtain wind and solar resource data for each individual location and to determine the hourly generation profile of a wind or solar plant over the course of a year based on NREL's Wind Integration National Dataset (WIND Toolkit)⁹⁹ for wind and the NREL National Solar Resource Database (NSRDB)¹⁰⁰ for solar PV. We oversize the wind plant by 8.1% to account for wind turbine power output degradation, which Hamilton et al.¹⁰¹ estimated at 0.27% per year. The off-grid wind + solar + battery production route also includes 1 h of Li-ion battery storage duration at 15% of electrolyzer beginning-of-life capacity to assist in black starts and help mitigate sub-hourly variations in wind and solar plant output.

We also assume that electrolyzer power electronics are oversized by 13% to manage a corresponding increase in the required electrolyzer stack voltage to maintain the same hydrogen production capacity by the end of the stack's life.⁹⁴ The PEM electrolyzer model within HOPP accounts for stack degradation over the life of each stack, effectively capturing the reduction in stack efficiency caused by degradation associated with steady-state operation, dynamic operation, and on-off switching.⁷⁰ To calculate the hydrogen storage capacity for off-grid electrolysis production routes, the model first solves a state-of-charge calculation throughout 1 year of operation based on the hourly hydrogen production profile and an assumed flat hourly demand profile for the steel or ammonia facility. The framework calculates the total required hydrogen storage capacity by subtracting the minimum state of charge from the maximum state of charge.

The renewable and battery technology costs were obtained from NREL's^{98,100} Annual Technology Baseline (ATB) moderate scenarios.¹⁰² The capital and operating costs for the wind and solar plants in each studied year and location are summarized in Table S11, and Table S12 gives the lithium-ion battery costs.

Electrolyzer system layout, operation, and cost methodology

The largest installed PEM electrolyzer system to date is 20 MW in capacity¹⁰³; hence, PEM electrolysis systems at the scale presented in this study are unprecedented. Previous analyses have been performed to assess the characteristics of potential gigawatt-scale PEM electrolysis facilities. Most notably, the Institute for Sustainable Process Technology recently published a study that outlined 1-GW-scale AEL and PEM electrolyzers

that could potentially be brought online by 2030.¹⁰⁴ This study assumes that PEM electrolyzer stacks would be sized at 10 MW and clustered into individual subsystems (including medium-voltage transformers, rectifiers, hydrogen separation, and heat exchangers) sized at 40 MW. We follow this approach within our study, assuming that electrolyzer systems must be sized in multiples of 40 MW to take advantage of economies of scale of purchasing balance-of-plant equipment at that capacity. We also assume that the maximum number of independently operable electrolyzer stack clusters is determined as the total system capacity divided by 40. This assumption factors into stack cluster control and the amount of power below 15% of the electrolyzer rating that the electrolysis system can capture. Above 15% of rated electrolysis system capacity, the model splits power equally across all stack clusters to maximize efficiency. Below 15% of rated system electrolysis capacity but above 15% of single cluster capacity (which works out to 6 MW for a 40 MW stack cluster), the model calculates the maximum number of stack clusters that can operate while remaining above 15% of cluster capacity and randomly selects clusters to operate at the corresponding load. Below 15% of cluster capacity, the model turns off all electrolysis stack clusters, and any wind or solar power produced during that period is curtailed. The modeling framework keeps track of the impact of stack cluster on-off cycling on individual stack cluster life and calculates average stack cluster lifetimes that ProFAST then uses to assign a stack replacement schedule and calculate the associated refurbishment costs. The approach described above maximizes efficiency at the potential expense of more stack on-off cycling and associated degradation, although to some extent these effects balance out because the primary impact of degradation is to reduce efficiency. More detailed optimization of stack optimization considering degradation is a complex and important field area of research but beyond the scope of the present analysis.

Because this study aims to quantify electrolyzer costs under different potential future scenarios, it is valuable to employ subsystem scaling factors and learning rates when estimating costs. Subsystem scaling factors capture differences in economies of scale for individual subsystems, enabling a more detailed assessment of how electrolyzer system costs might scale with changes in subsystem capacity. Employing subsystem learning rates allows for the identification of how different subsystems will reduce in cost at different rates as the technology becomes more widely deployed. In this study, we employ the scaling factors and learning rates used by Böhm et al.¹⁸ with the current system cost status from DOE's Hydrogen and Fuel Cell Technologies Office (HFTO)²² and future electrolyzer cost projections and targets from DOE's Office of Clean Energy Demonstrations¹⁴ and HFTO²², respectively. Note S2 provides more details regarding the electrolyzer cost methodology, and Tables S14–S19 provide specific values.

Retail electricity price projection methodology

Previous studies that have investigated grid-powered electrolysis often use actual data for wholesale and TOU or RTP rate structures.^{87–89} These studies have demonstrated that with current electrolyzer and above-ground hydrogen storage costs and

with current rate structures, grid connectivity generally results in lower hydrogen production costs than off-grid (islanded) systems. Analysis of future electrolysis-based hydrogen production for large-scale industrial customers such as steel and ammonia plants, however, requires a different set of assumptions. Although some large-scale industrial electricity consumers have access to wholesale electricity rates,^{105,106} it is unclear from publicly available data how widespread this access is and/or if it will become more widespread in the future. Second, though TOU and RTP structures do exist for industrial electricity consumers, it is unclear how many actually take advantage of these structures. Most electricity customers in the US receive annually or seasonally fixed rates,^{107–110} and the EIA recently estimated that only 7.3% of all customers (including residential, commercial, and industrial) currently take advantage of time-varying rate structures.¹¹⁰ Further, though it is fairly easy to find current time-varying industrial retail rate structures, it is very difficult to predict how utilities will structure future retail rates, particularly in the context of deeply decarbonized future grids. Many components of retail prices are omitted in power system planning studies,¹¹¹ and regional prices are difficult to predict because of various issues, such as congestion in regional transmission lines.¹¹² Further exploration of future time-varying rate structures and their impacts on the economics of grid-powered electrolysis would be valuable but is outside the scope of this analysis.

For these reasons, we take a simplified approach in estimating the potential range of future industrial consumer grid prices for a deeply decarbonized electric grid. To account for the uncertainty in future industrial retail price projections, we consider low and medium retail grid price scenarios. In the low grid price scenario, we assume that retail rates are consistent with the annual average wholesale prices from NREL's Cambium 2022 database Mid-case 100% Decarbonization by 2035 scenario. We estimate the retail prices for the mid-case scenario using the following steps:

- (1) obtain the annual average retail prices for 2022 from the EIA AEO 2022⁸⁶ for each region of interest;
- (2) calculate the average annual wholesale rates for each region of interest using NREL's Cambium 2022 database Mid-case 100% Decarbonization by 2035 scenario;
- (3) calculate the difference between the AEO 2022 annual average retail rate and the Cambium average annual wholesale rate to obtain the regional wholesale markup;
- (4) apply the regional 2022 wholesale rate markup to the average annual wholesale rate estimated by Cambium for each fifth subsequent analysis year (Cambium 2022 has a temporal resolution of 5 years) to get the estimated retail rate—this assumes that administrative and business costs that account for retail rate markup are constant over time;
- (5) calculate a moving average rate for each year based on a weighted average. The weights assigned are 40% for the year in question and 30% each for the data 5 years prior and 5 years after the year in question; and
- (6) temporally interpolate the retail rates in each region to obtain the retail rates for the years not explicitly represented in Cambium.

Table S21 gives the resulting retail prices calculated for each year and each location. Also, note the difference between technology year and commissioning year. Many plots shown in the **results** section are for a given technology year, which indicates the year that the project is initiated and the generation of technologies selected for that project. Here, we assume that plants are brought online approximately 5 years later, and as a result, the first retail rate year occurs 5 years after a given technology year. We assume that each plant uses the same amount of grid electricity each year of its operation, with additional electricity allocated to account for electrolyzer cell stack degradation. We apply the changing grid prices throughout the plant's life by interpolating the data in **Table S21** up to 2050, and we subsequently assume that prices remain constant at the 2050 values beyond that point.

LCA methodology

The LCA performed in this work accounts for CO₂, methane, and nitrous oxide and covers all well-to-gate emissions. This entails considering indirect emissions from extracting and processing the raw materials and manufacturing the equipment (scope 3), indirect emissions from power generation (scope 2), and direct emissions from the hydrogen, ammonia, and steel production processes themselves (scope 1). We calculate the life-cycle emissions for each process, capturing the GHG emissions for each unit of hydrogen, steel, and ammonia for the entire duration of the plant life (30 years). Scopes 2 and 3 grid emissions intensity data come from NREL's Cambium 2022 database⁴³ Mid-case 100% Decarbonization by 2035 scenario. The data are evaluated for electrolysis cases on an hourly basis, considering when electrolyzers draw electricity from the grid (grid-only production routes continuously draw electricity from the grid, but hybrid-grid production routes only pull enough electricity from the grid to supplement on-site renewable production). The remaining emissions intensity data, including direct and upstream emissions for steel and ammonia production and embodied emissions for all technologies, are from ANL's GREET (2022) model.⁷⁶ The total emissions intensity for hydrogen, steel, and ammonia is calculated by summing the emissions intensities of the respective scopes 3, 2, and 1 emissions of each production route. **Tables S23–S25** provide the LCA assumptions used in this study.

RESOURCE AVAILABILITY

Lead contact

Further information and requests for resources and materials should be directed to and will be fulfilled by the lead contact, Jennifer King (Jennifer.King@nrel.gov).

Materials availability

No materials were generated in this study.

Data and code availability

- All original code has been deposited at Zenodo for the HOPP model and the mathematical framework that runs HOPP. Both are publicly available as of the date of the publication: HOPP Zenodo Database: <https://doi.org/10.5281/zenodo.14635565>; Mathematical framework Zenodo Database: <https://doi.org/10.5281/zenodo.14635575>.
- Running the framework also requires the NREL model "ProFAST," which can be found on Github. ProFAST Github Database: <https://github.com/nrel/profast/>.

- A newer version of HOPP can also be found on Github. HOPP Github Database: <https://github.com/nrel/hopp/>.

ACKNOWLEDGMENTS

This work was authored by the National Renewable Energy Laboratory, operated by Alliance for Sustainable Energy, LLC, Lawrence Berkeley National Laboratory, Argonne National Laboratory, and Oak Ridge National Laboratory for the US Department of Energy (DOE) under respective contract nos. DE-AC36-08GO28308, DE-AC02-05CH11231, DE-AC02-06CH11357, and DE-AC05-00OR22725. Funding was provided by the Hydrogen and Fuel Cell Technologies Office and the Wind Energy Technologies Office within the US Department of Energy's Office of Energy Efficiency and Renewable Energy. The views expressed in the article do not necessarily represent the views of the DOE or the US Government. The US Government retains, and the publisher, by accepting the article for publication, acknowledges that the US Government retains a nonexclusive, paid-up, irrevocable, worldwide license to publish or reproduce the published form of this work, or allow others to do so, for US Government purposes.

The authors acknowledge the assistance of their colleagues from the National Energy Technology Laboratory (NETL), in particular Dr. David Morgan, who provided guidance and support in deriving the CO₂ storage costs in this work.

AUTHOR CONTRIBUTIONS

Conceptualization, J.K., S.H., R.T., E.A., H.B., and J.O.P.P.; methodology, E.P.R., M.N.K., J.K., M.K., E.G., S.V., K.B., J.T., A.G., V.S., P.S., K.L., A.E., H.B., and F.R.; software, E.P.R., M.N.K., M.K., E.G., S.V., K.B., J.T., and A.G.; formal analysis, E.P.R., M.N.K., and E.G.; data curation, E.P.R., M.N.K., J.K., M.K., E.G., S.V., K.B., A.G., P.S., K.L., and F.R.; writing – original draft, E.P.R., M.N.K., J.K., M.K., and E.G.; writing – review and editing, E.P.R., M.N.K., J.K., M.K., K.B., S.B., R.T., P.S., K.L., A.E., H.B., F.R., and J.P.P.; visualization, E.P.R., E.G., and K.B.; supervision, J.K., S.K., R.T., A.E., and H.B.; project administration, J.K., S.K., R.T., A.E., and H.B.; funding acquisition, J.K., S.K., R.T., A.E., and H.B.

DECLARATION OF INTERESTS

The authors declare no competing interests.

SUPPLEMENTAL INFORMATION

Supplemental information can be found online at <https://doi.org/10.1016/j.jrs.2025.100338>.

Received: November 21, 2024

Revised: January 12, 2025

Accepted: February 4, 2025

Published: March 14, 2025

REFERENCES

1. EPA. (2023). Inventory of U.S. Greenhouse Gas Emissions and Sinks: 1990–2021. Tech. Rep. EPA 430-R-23-002. <https://www.epa.gov/system/files/documents/2023-04/US-GHG-Inventory-2023-Main-Text.pdf>.
2. World Steel Association. (2023). Climate change and the production of iron and steel. <https://worldsteel.org/publications/policy-papers/climate-change-policy-paper/>.
3. Devlin, A., Kossen, J., Goldie-Jones, H., and Yang, A. (2023). Global green hydrogen-based steel opportunities surrounding high quality renewable energy and iron ore deposits. Nat. Commun. 14, 2578. <https://doi.org/10.1038/s41467-023-38123-2>.
4. IEA. (2020). Global crude steel production by process route and scenario, 2019–2050. <https://www.iea.org/data-and-statistics/charts/global-crude-steel-production-by-process-route-and-scenario-2019-2050>.

5. American Iron and Steel Institute. (2023). AISI releases annual statistical report for 2022. <https://www.steel.org/2023/06/aisi-releases-annual-statistical-report-for-2022/>.
6. Terry, J., Gamage, C., Yavorsky, N., and Wilmoth, R. (2023). Unlocking the First Wave of Breakthrough Steel Investments in the United States. Tech. Rep. <https://rmi.org/insight/unlocking-first-wave-of-breakthrough-steel-investments-in-the-united-states/>.
7. International Energy Agency. (2022). Iron and Steel. <https://www.iea.org/reports/iron-and-steel>.
8. Zang, G., Sun, P., Elgowainy, A., Bobba, P., McMillan, C., Ma, O., Podkaminer, K., Rustagi, N., Melaina, M., and Koleva, M. (2023). Cost and Life Cycle Analysis for Deep CO₂ Emissions Reduction for Steel Making: Direct Reduced Iron Technologies. *Steel Res. Int.* 94, 2200297. <https://doi.org/10.1002/srin.202200297>.
9. The Royal Society. (2020). Ammonia: zero-carbon fertiliser, fuel and energy store. Policy Briefing. Tech. Rep. <https://royalsociety.org/-/media/policy/projects/green-ammonia/green-ammonia-policy-briefing.pdf>.
10. Statista. (2023). Ammonia production in the United States from 2014 to 2022. <https://www.statista.com/statistics/982841/us-ammonia-production/>.
11. S&P Global (2020). Chemical Economics Handbook: Ammonia. <https://www.spglobal.com/commodityinsights/en/ci/products/ammonia-chemical-economics-handbook.html>.
12. Decarbonization Technology. (2023). Hydrogen derivatives key to the global renewable energy trade. <https://decarbonisationtechnology.com/article/188/hydrogen-derivatives-key-to-the-global-renewable-energy-trade>.
13. U.S. Department of Energy. (2006). Potential Roles of Ammonia in a Hydrogen Economy. <https://www.energy.gov/eere/fuelcells/articles/potential-roles-ammonia-hydrogen-economy>.
14. U.S. Department of Energy. (2023). Pathways to Commercial Liftoff: Clean Hydrogen. Tech. Rep. <https://liftoff.energy.gov/wp-content/uploads/2023/05/20230523-Pathways-to-Commercial-Liftoff-Clean-Hydrogen.pdf>.
15. International Renewable Energy Agency. (2022). Renewable Power Generation. Costs in 2021. https://www.irena.org/-/media/Files/IRENA/Agency/Publication/2022/Jul/IRENA_Power_Generation_Costs_2021.pdf?rev=34c22a4b244d434da0accde7de7c73d8.
16. International Energy Agency. (2021). Net Zero by 2050. A Roadmap for the Global Energy Sector. https://iea.blob.core.windows.net/assets/deebef5d-0c34-4539-9d0c-10b13d840027/NetZeroby2050-ARoadmapfortheGlobalEnergySector_CORR.pdf.
17. Böhm, H., Goers, S., and Zauner, A. (2019). Estimating future costs of power-to-gas – a component-based approach for technological learning. *Int. J. Hydrot. Energy* 44, 30789–30805. <https://doi.org/10.1016/j.ijhydene.2019.09.230>.
18. Böhm, H., Zauner, A., Rosenfeld, D.C., and Tichler, R. (2020). Projecting cost development for future large-scale power-to-gas implementations by scaling effects. *Appl. Energy* 264, 114780. <https://doi.org/10.1016/j.apenergy.2020.114780>.
19. Glenk, G., Holler, P., and Reichelstein, S. (2023). Advances in power-to-gas technologies: Cost and conversion efficiency. TRR 266 Accounting for Transparency Working Paper. *Energy Environ. Sci.* 109, 6058–6070. <https://doi.org/10.1039/D3EE01208E>.
20. Schmidt, O., Melchior, S., Hawkes, A., and Staffell, I. (2019). Projecting the Future Levelized Cost of Electricity Storage Technologies. *Joule* 3, 81–100. <https://doi.org/10.1016/j.joule.2018.12.008>.
21. Badgett, A., Brauch, J., Thatte, A., Rubin, R., Skangos, C., Wang, X., Ahluwalia, R., Pivovar, B., and Ruth, M. (2024). Updated Manufactured Cost Analysis for Proton Exchange Membrane Water Electrolyzers. Tech. Rep. <https://www.nrel.gov/docs/fy24osti/87625.pdf>
22. HFTO. (2023). Technical Targets for Proton Exchange Membrane Electrolysis. <https://www.energy.gov/eere/fuelcells/technical-targets-proton-exchange-membrane-electrolysis>.
23. HFTO. (2023). Technical Targets for Liquid Alkaline Electrolysis. <https://www.energy.gov/eere/fuelcells/technical-targets-liquid-alkaline-electrolysis>.
24. Danish Energy Agency. (2024). Renewable fuels: Technology descriptions and projections for long-term energy system planning. Version 12. Tech. Rep. https://ens.dk/sites/ens.dk/files/Analyser/technology_data_for_renewable_fuels.pdf.
25. IRS. (2022). Credits and Deductions Under the Inflation Reduction Act of 2022. <https://www.irs.gov/credits-and-deductions-under-the-inflation-reduction-act-of-2022>.
26. Ruth, M.F., Jadun, P., Gilroy, N., Connelly, E., Boardman, R., Simon, A., Elgowainy, A., and Zuboy, J. (2020). The Technical and Economic Potential of the H2@Scale Concept within the United States. Tech. Rep. NREL/TP-6A20-77610. <https://www.nrel.gov/docs/fy21osti/77610.pdf>.
27. Fischbeck, M., Marzinkowski, J., Winzer, P., and Weigel, M. (2014). Techno-economic evaluation of innovative steel production technologies. *J. Cleaner Prod.* 84, 563–580. <https://doi.org/10.1016/j.jclepro.2014.05.063>.
28. Fan, Z., and Friedmann, S.J. (2021). Low-carbon production of iron and steel: Technology options, economic assessment, and policy. *Joule* 5, 829–862. <https://doi.org/10.1016/j.joule.2021.02.018>.
29. Vogl, V., Åhman, M., and Nilsson, L.J. (2018). Assessment of hydrogen direct reduction for fossil-free steelmaking. *J. Cleaner Prod.* 203, 736–745. <https://doi.org/10.1016/j.jclepro.2018.08.279>.
30. Toktarova, A., Göransson, L., and Johnsson, F. (2021). Design of clean steel production with hydrogen: Impact of electricity system composition. *Energies* 14, 8349. <https://doi.org/10.3390/en14248349>.
31. Campion, N., Nami, H., Swisher, P.R., Vang Hendriksen, P., and Münster, M. (2023). Techno-economic assessment of green ammonia production with different wind and solar potentials. *Renew. Sustain. Energy Rev.* 173, 113057. <https://doi.org/10.1016/j.rser.2022.113057>.
32. Marocco, P., Gandiglio, M., Audisio, D., and Santarelli, M. (2023). Assessment of the role of hydrogen to produce high-temperature heat in the steel industry. *J. Cleaner Prod.* 388, 135969. <https://doi.org/10.1016/j.jclepro.2023.135969>.
33. Sousa, J., Waiblinger, W., and Friedrich, K.A. (2022). Techno-economic study of an electrolysis-based green ammonia production plant. *Ind. Eng. Chem. Res.* 61, 14515–14530. <https://doi.org/10.1021/acs.iecr.2c00383>.
34. Mayer, P., Ramirez, A., Pezzella, G., Winter, B., Sarathy, M., Gascon, J., and Bardow, A. (2022). Blue vs. Green Ammonia Production: A Techno-Economic and Life Cycle Assessment Perspective. *iScience* 26, 107389. <https://doi.org/10.2139/ssrn.4309114>.
35. Rosner, F., Papadias, D.D., Brooks, K.P., Yoro, K., Ahluwalia, R.K., Autrey, T., and Breunig, H. (2023). Green steel: design and cost analysis of hydrogen-based direct iron reduction. *Energy Environ. Sci.* 16, 4121–4134. <https://doi.org/10.1039/D3EE01077E>.
36. D'Angelo, S.C., Cobo, S., Tulus, V., Nabera, A., Martín, A.J., Pérez-Ramírez, J., and Guillén-Gosálbez, G. (2021). Planetary boundaries analysis of low-carbon ammonia production routes. *ACS Sustainable Chem. Eng.* 9, 9740–9749. <https://doi.org/10.1021/acssuschemeng.1c01915>.
37. Suer, J., Traverso, M., and Jäger, N. (2022). Carbon footprint assessment of hydrogen and steel. *Energies* 15, 9468. <https://doi.org/10.3390/en15249468>.
38. Nurdawati, A., Zaini, I.N., Wei, W., Gyllenram, R., Yang, W., and Samuelsson, P. (2023). Towards fossil-free steel: Life cycle assessment of biosyngas-based direct reduced iron (DRI) production process. *J. Cleaner Prod.* 393, 136262. <https://doi.org/10.1016/j.jclepro.2023.136262>.
39. Statista. (2024). Ammonia plant production capacity in the United States in 2022, by facility. <https://www.statista.com/statistics/1266392/ammonia-plant-capacities-united-states/>.
40. Statista. (2024). Steel production figures in the U.S. from 2006 to 2022. <https://www.statista.com/statistics/209343/steel-production-in-the-us/>.

41. Global Energy Monitor (2023). Green Steel Plant Tracker. Summary Tables. <https://globalenergymonitor.org/projects/global-steel-plant-tracker/summary-tables/>.
42. Department of the Treasury. (2023). Section 45V Credit for Production of Clean Hydrogen; Section 48(a)15 Election To Treat Clean Hydrogen Production Facilities as Energy Property. <https://www.govinfo.gov/content/pkg/FR-2023-12-26/pdf/2023-28359.pdf>.
43. National Renewable Energy Laboratory. (2023). Cambium. <https://www.nrel.gov/analysis/cambium.html>.
44. Getty Images (2023). Wind turbines line art icon - stock illustration. <https://www.gettyimages.com/detail/illustration/wind-turbines-line-art-icon-royalty-free-illustration/1303567210?adppopup=true>.
45. Getty Images (2023). Electric tower icon set - stock illustration. <https://www.gettyimages.com/detail/illustration/electric-tower-icon-set-royalty-free-illustration/1337649626?adppopup=true>.
46. Getty Images (2023). Carbon dioxide line icon - stock illustration. <https://www.gettyimages.com/detail/illustration/carbon-dioxide-line-icon-royalty-free-illustration/1555533327?adppopup=true>.
47. Phoenix Equipment Corporation. (2022). Buyer and Seller of Process Equipment and Process Plants – Phoenix Equipment. <https://www.phxequip.com/>.
48. DreamsTime. (2022). 3d arc furnace steel icon. <https://www.dreamstime.com/stock-illustration-d-arc-furnace-steel-icon-image-image41305609>.
49. Papadias, D.D., and Ahluwalia, R.K. (2021). Bulk storage of hydrogen. *Int. J. Hydrol. Energy* 46, 34527–34541. <https://doi.org/10.1016/j.ijhydene.2021.08.028>.
50. Derking, H., van der Togt, L., and Keezer, M. (2019). Liquid Hydrogen Storage: Status and Future Perspectives. <https://www.utwente.nl/en/tnw/ems/research/ats/Events/chmrt/m13-hendrie-derking-cryoworld-chmrt-2019.pdf>.
51. Petitpas, G. (2018). Boil-off losses along LH₂ pathway. <https://www.osti.gov/servlets/purl/1466121>.
52. DeSantis, D., James, B.D., Houchins, C., Saur, G., and Lyubovsky, M. (2021). Cost of long-distance energy transmission by different carriers. *iScience* 24, 103495. <https://doi.org/10.1016/j.isci.2021.103495>.
53. U.S. Department of Energy. (2020). Department of Energy Hydrogen Program Plan. Tech. Rep. DOE/EE-2128. <https://www.hydrogen.energy.gov/pdfs/hydrogen-program-plan-2020.pdf>.
54. DOE Hydrogen and Fuel Cell Technologies Office. (2021). Hydrogen Pipelines. <https://www.energy.gov/eere/fuelcells/hydrogen-pipelines>.
55. Argonne National Laboratory. (2023). HYDROGEN DELIVERY SCENARIO ANALYSIS MODEL (HDSAM). <https://hdsam.es.anl.gov/index.php?content=hdsam>.
56. United States Steel. (2023). Locations: U.S. Steel's Footprint. <https://www.ussteel.com/about-us/locations>.
57. Environmental Protection Agency. (2016). Iron and Steel. <https://archive.epa.gov/sectors/web/html/steel.html>.
58. Minnesota Department of Natural Resources Division of Lands and Minerals. (2016). Explore Minnesota: Iron Ore. https://files.dnr.state.mn.us/lands_minerals/mcc_docs/2016_explore_iron_ore.pdf.
59. Pisciotta, M., Pilorgé, H., Feldmann, J., Jacobson, R., Davids, J., Swett, S., Sasso, Z., and Wilcox, J. (2022). Current state of industrial heating and opportunities for decarbonization. *Prog. Energy Combust. Sci.* 91, 100982. <https://doi.org/10.1016/j.pecs.2021.100982>.
60. NuStar. (2021). Pipeline Transportation of Ammonia. Helping to Bridge the Gap to a Carbon Free Future. <https://www.ammoniaenergy.org/wp-content/uploads/2021/11/AEA-Ammonia-Pipeline-Transportation-MEA-11-4-2021.pdf>.
61. NREL. (2023). reV: The Renewable Energy Potential Model. <https://www.nrel.gov/gis/renewable-energy-potential.html>.
62. NREL. (2020). Hybrid Energy Systems Research. <https://www.nrel.gov/wind/hybrid-energy-systems-research.html>.
63. Roy, A., Watson, S., and Infield, D. (2006). Comparison of electrical energy efficiency of atmospheric and high-pressure electrolyzers. *Int. J. Hydrol. Energy* 31, 1964–1979. <https://doi.org/10.1016/j.ijhydene.2006.01.018>.
64. Yigit, T., and Selamet, O.F. (2016). Mathematical modeling and dynamic Simulink simulation of high-pressure PEM electrolyzer system. *Int. J. Hydrol. Energy* 41, 13901–13914. <https://doi.org/10.1016/j.ijhydene.2016.06.022>.
65. Tebibel, H., and Medjebeur, R. (2018). Comparative performance analysis of a grid connected PV system for hydrogen production using PEM water, methanol and hybrid sulfur electrolysis. *Int. J. Hydrol. Energy* 43, 3482–3498. <https://doi.org/10.1016/j.ijhydene.2017.12.084>.
66. Salami Tijani A., Abdol Rahim A.H., Badrol Hisam M.K. A study of the loss characteristic of a high pressure electrolyzer system for hydrogen production. *J. Teknol.* 2015;75(8):65–69. doi:10.11113/jt.v75.5213.
67. Ruuskanen, V., Koponen, J., Huoman, K., Kosonen, A., Niemelä, M., and Ahola, J. (2017). PEM water electrolyzer model for a power-hardware-in-loop simulator. *Int. J. Hydrol. Energy* 42, 10775–10784. <https://doi.org/10.1016/j.ijhydene.2017.03.046>.
68. García-Valverde, R., Espinosa, N., and Urbina, A. (2012). Simple PEM water electrolyser model and experimental validation. *Int. J. Hydrol. Energy*. 10th International Conference on Clean Energy 2010 37, 1927–1938. <https://doi.org/10.1016/j.ijhydene.2011.09.027>.
69. Shiva Kumar, S., and Himabindu, V. (2019). Hydrogen production by PEM water electrolysis – A review. *Mater. Sci. Energy Technol.* 2, 442–454. <https://doi.org/10.1016/j.mset.2019.03.002>.
70. Tully, Z., Starke, G., Johnson, K., and King, J. (2023). An Investigation of Heuristic Control Strategies for Multi-Electrolyzer Wind-Hydrogen Systems Considering Degradation. In 2023 IEEE Conference on Control Technology and Applications (CCTA) (IEEE), pp. 817–822. <https://doi.org/10.1109/CCTA54093.2023.10252187>.
71. Badgett, A., Brauch, J., Saha, P., and Pivovar, B. (2024). Decarbonization of the Electric Power Sector and Implications for Low-Cost Hydrogen Production from Water Electrolysis. *Adv. Sustain. Syst.* 8, 2300091. <https://doi.org/10.1002/adsu.202300091>.
72. Wang, X., Star, A.G., and Ahluwalia, R.K. (2023). Performance of Polymer Electrolyte Membrane Water Electrolysis Systems: Configuration, Stack Materials, Turndown and Efficiency. *Energies* 16, 4964. <https://doi.org/10.3390/en16134964>.
73. Mallapragada, D.S., Gençer, E., Insinger, P., Keith, D.W., and O'Sullivan, F.M. (2020). Can Industrial-Scale Solar Hydrogen Supplied from Commodity Technologies Be Cost Competitive by 2030? *Physiol. Sci.* 1, 100174. <https://doi.org/10.1016/j.xcpr.2020.100174>.
74. Kee, J., and Penev, M.M. (2023). ProFAST (Production Financial Analysis Scenario Tool) [SWR-23-88]. <https://doi.org/10.11578/dc.20231211.1>.
75. NREL. (2022). H2FAST: Hydrogen Financial Analysis Scenario Tool. <https://www.nrel.gov/hydrogen/h2fast.html>.
76. Argonne National Laboratory. (2023). GREET. <https://greet.es.anl.gov/>.
77. Greenhouse Gas Protocol (2011). Sector Toolsets for Iron and Steel—Guidance Document. <https://ghgprotocol.org/>.
78. Lee, K., Liu, X., Vyawahare, P., Sun, P., Elgowainy, A., and Wang, M. (2022). Techno-economic performances and life cycle greenhouse gas emissions of various ammonia production pathways including conventional, carbon-capturing, nuclear-powered, and renewable production. *Green Chem.* 24, 4830–4844. <https://doi.org/10.1039/D2GC00843B>.
79. Congress.Gov. (2022). H.R.5376 - Inflation Reduction Act of 2022. <https://www.congress.gov/bill/117th-congress/house-bill/5376/text>.
80. U.S. Department of the Treasury. (2025). U.S. Department of the Treasury Releases Final Rules for Clean Hydrogen Production Tax Credit. <https://home.treasury.gov/news/press-releases/jy2768>.
81. MIDREX. (2022). MIDREX NG with H₂ Addition: moving from natural gas to hydrogen in decarbonizing ironmaking. <https://www.midrex.com/tech-article/moving-from-natural-gas-to-hydrogen-in-decarbonizing-ironmaking/>.

82. Wu, S., Salmon, N., Li, M.M.J., Bañares-Alcántara, R., and Tsang, S.C.E. (2022). Energy Decarbonization via Green H₂ or NH₃? ACS Energy Lett. 7, 1021–1033. <https://doi.org/10.1021/acsenergylett.1c02816>.
83. IRENA and Ammonia Energy Association. (2022). INNOVATION OUTLOOK. RENEWABLE AMMONIA. https://www.irena.org/-/media/Files/IRENA/Agency/Publication/2022/May/IRENA_Innovation_Outlook_Ammonia_2022.pdf.
84. Rosbo, J.W., Ritschel, T.K.S., Hørsholt, S., Huusom, J.K., and Jørgensen, J.B. (2023). Flexible operation, optimisation and stabilising control of a quench cooled ammonia reactor for power-to-ammonia. Comput. Chem. Eng. 176, 108316. <https://doi.org/10.1016/j.compchemeng.2023.108316>.
85. Bagga, K. (2021). Flexible green ammonia synthesis and large scale ammonia cracking technology by Uhde®. <https://www.ammoniaenergy.org/wp-content/uploads/2021/09/thyssenkruppUhde-FlexibleGreenAmmoniaSynthesisCracking-r00.pdf>.
86. EIA. (2023). Annual Energy Outlook 2023. <https://www.eia.gov/outlooks/aoe/data/browser/>.
87. Eichman, J., Koleva, M., Guerra, O.J., and McLaughlin, B. (2020). Optimizing an Integrated Renewable-Electrolysis System. Tech. Rep. NREL/TP-5400-75635 NREL. <https://www.nrel.gov/docs/fy20osti/75635.pdf>.
88. Koleva, M., Guerra, O.J., Eichman, J., Hodge, B.M., and Kurtz, J. (2021). Optimal design of solar-driven electrolytic hydrogen production systems within electricity markets. J. Power Sources 483, 229183. <https://doi.org/10.1016/j.jpowsour.2020.229183>.
89. Fernández, G., José, O., Eichman, J., Hurlbut, D.J., and Xu, K. (2022). Integrating Hydrogen Production and Electricity Markets: Analytica Insights from California. Tech. Rep. NREL/TP-6A40-80902 NREL. <https://www.nrel.gov/docs/fy22osti/80902.pdf>.
90. Jalving, J., Ghose, J., Cortes, N., Gao, X., Kenuven, B., Agi, D., Martin, S., Chen, X., Guillet, D., Tumbalam-Gooty, R., et al. (2023). Beyond price taker: Conceptual design and optimization of integrated energy systems using machine learning market surrogates. Appl. Energy 351, 121767. <https://doi.org/10.1016/j.apenergy.2023.121767>.
91. National Energy Technology Laboratory. (2017). FE/NETL CO₂ Saline Storage Cost Model (2017). <https://edx.netl.doe.gov/dataset/fe-netl-co2-saline-storage-cost-model-2017>.
92. ProSim. (2023). ProSim. Software & Services in Process Simulation. <https://www.prosim.net/en/>.
93. Bureau of Transportation Statistics. (2023). Average Freight Revenue per Ton-Mile. <https://www.bts.gov/content/average-freight-revenue-ton-mile>.
94. NREL. (2022). H2A: Hydrogen Analysis Production Models. <https://www.nrel.gov/hydrogen/h2a-production-models.html>.
95. National Energy Technology Laboratory. (2023). FECM/NETL CO₂ Transport Cost Model (2023). <https://netl.doe.gov/energy-analysis/details?id=d3086f60-278d-4e97-a649-8e4d5ce5e93c>.
96. U.S. Energy Information Administration. (2023). Annual Energy Outlook 2023. <https://www.eia.gov/outlooks/aoe/data/browser/>.
97. Eberle, A., Mai, T., Lopez, A., Pinchuk, P., Williams, T., Roberts, O., Stehly, T., Buster, G., Mowers, M., Lantz, E., and Stanley, P. (2024). Incorporating Wind Turbine Choice in High-Resolution Geospatial Supply Curve and Capacity Expansion Models. <https://www.nrel.gov/docs/fy24osti/87161.pdf>.
98. NREL. (2024). PySAM. <https://nrel-pysam.readthedocs.io/en/main/>.
99. NREL. (2023). Wind Integration National Dataset Toolkit. <https://www.nrel.gov/grid/wind-toolkit.html>.
100. NREL. (2024). NSRDB: National Solar Radiation Database. <https://nsrdb.nrel.gov/>.
101. Hamilton, S.D., Millstein, D., Bolinger, M., Wiser, R., and Jeong, S. (2020). How Does Wind Project Performance Change with Age in the United States? Joule 4, 1004–1020. <https://doi.org/10.1016/j.joule.2020.04.005>.
102. National Renewable Energy Laboratory. (2024). Annual Technology Baseline. <https://atb.nrel.gov/>.
103. Air Liquide. (2021). Inauguration of the world's largest PEM electrolyzer to produce decarbonized hydrogen. <https://www.airliquide.com/stories/industry/inauguration-worlds-largest-pem-electrolyzer-produces-decarbonized-hydrogen>.
104. Institute for Sustainable Process Technology. (2022). A one-gigawatt green-hydrogen plant. advanced design and total installed-capital costs. Tech. Rep. <https://ispt.eu/media/Public-report-gigawatt-advanced-green-electrolyser-design.pdf>.
105. Ashton, L. (2022). Understanding Electric Rates Using FERC Data. HDATA. <https://blog.hdata.us/understanding-electric-rates-using-erc-data>.
106. Diversify. (2022). Everything You Need To Know About Wholesale Power Markets. <https://diversify.com/energy-brokers/wholesale-electricity-market-explained/>.
107. Borenstein, S., and Holland, S.P. (2005). On the Efficiency of Competitive Electricity Markets With Time-Invariant Retail Prices. J. Econ. 36, 469–493. <http://faculty.haas.berkeley.edu/borenste/download/Rand05RTP.pdf>.
108. PJM. (2017). Price Responsive Demand. <https://www.pjm.com/~/media/about-pjm/newsroom/fact-sheets/price-responsive-demand.ashx>.
109. ISO New England (2023). Wholesale vs. Retail Electricity Costs. <https://www.iso-ne.com/about/what-we-do/in-depth/wholesale-vs-retail-electricity-costs>.
110. Schittekatte, T., Mallapragada, D., Joskow, P.L., and Schmalensee, R. (2023). Economy-Wide Decarbonization Requires Fixing Retail Electricity Rates. MIT Center for Energy and Environmental Policy Research.
111. Brown, P.R., Gagnon, P.J., Corcoran, J.S., and Cole, W.J.. (2022). Retail Rate Projections for Long-Term Electricity System Models. Tech. Rep. NREL/TP-6A20-78224 NREL. <https://www.nrel.gov/docs/fy22osti/78224.pdf>.
112. Xu, J., Hu, B., Zhang, P., Zhou, X., Xing, Z., and Hu, Z. (2023). Regional electricity market price forecasting based on an adaptive spatial-temporal convolutional network. Front. Energy Res. 11, 1168944. <https://doi.org/10.3389/fenrg.2023.1168944>.